Methylmercury dietary pathways and bioaccumulation in benthic invertebrates of the Arctic Ocean

by

Christine M^{c}Clelland

A thesis submitted to the Faculty of Graduate and Postdoctoral Affairs

in partial fulfillment of the requirements for the degree of

Master of Science

In

Biology

Carleton University

Ottawa, Ontario

General abstract

This study described methylmercury (MeHg) concentrations in a wide array of benthic invertebrates sampled from two locations in the Canadian Beaufort Sea (Arctic Ocean). I examined relationships between dietary indicators, specifically carbon, nitrogen and sulfur stable isotope ratios, fatty acid and fatty acid biomarker signatures, all in relation to MeHg concentrations of taxa identified using traditional taxonomy and genetic barcoding approaches. Methylmercury concentrations increased with trophic position (inferred from nitrogen stable isotope ratios), varied by feeding guild and were influenced by the type of energy sources supporting the food web. Higher MeHg concentrations were observed at a site closer to the outflow of the Mackenzie River. When accounting for the effect of feeding guild and dietary indicators, the results clearly indicated that location influenced MeHg accumulation in the benthic invertebrates. These results contribute valuable information for tracking MeHg dynamics in this region.

Acknowledgements

Freshly out of university for my B.Sc., I was fortuitously taken under the wing of Dr. Kathy Conlan (Canadian Museum of Nature) who gave me incredible opportunities and set me on a path I have treasured from the very beginning. With Kathy, I developed a love of polar ocean science, field work and marine invertebrates. Thank you Kathy for bringing me along as your field assistant all those years ago.

Within Environment and Climate Change Canada (ECCC), I found new professional purpose when I started working for Dr. John Chételat. John, your scientific expertise, patient guidance and thoughtfulness make you an outstanding research scientist, supervisor, collaborator and friend. I thank you and Dr. Mark Forbes for supporting me throughout this journey.

Mark, your uncanny ability to set people at ease while pushing them to succeed was very much appreciated. Thank you for agreeing to extend the realm of expertise even further to include Arctic benthic marine ecology and guide me through this process. I am indebted to Dr. Frances Pick and Dr. Stacey Robinson for their wisdom, guidance and encouragement. The support I found in the Robinson-Forbes lab group was invaluable to my passage through graduate school during a pandemic.

Finally, I would like to extend my gratitude to my manager Bruce Pauli for supporting my desire to develop my knowledge and research skills while also encouraging me to keep a healthy balance with my family life.

This research was initially funded by the Northern Scientific Training Program, Canadian Museum of Nature (CMN, Dr. Kathleen Conlan), the University of Saskatchewan (USask, Dr. Alec Aitken), the Department of Fisheries and Oceans (DFO, Don Cobb) and the Geological Survey of Canada (GSC, Dr. Steve Blasco) for the Northern Coastal Marine Studies Program. Further funding was received from Environment and Climate Change Canada (ECCC, Dr. John Chételat, Bruce Pauli).

For advice and logistical support of the invertebrate collections, I would like to thank the Fisheries Joint Management Committee of the Inuvialuit Settlement Region, Dr. Bill Williams (DFO), Dr. Chris Parrish (Memorial University), Aurora Research Institute (Inuvik), the Canadian Hydrographic Service and captain and crew of CCGS Nahidik (2007). For sample collecting assistance, I am grateful for the generosity and spirit of collaboration extended to me be Andy Majewski (DFO) and Brad Park (DFO), Megan Foss and Dr. Alec Aitken.

For chemical analyses, advice and support, I am grateful for the help I received from Dr. John Chételat, Dr. Craig Hebert, Michelle Zanuttig, Francois Cyr, Emily Porter, David Carpenter (ECCC, National Wildlife Research Centre), Dr. Mark Forbes (Carleton University), the Ján Veizer Stable Isotope Laboratory (Paul Middlestead, Wendy Abdi, Patricia Wickham, University of Ottawa), and Roger Bull (Laboratory of Molecular Biodiversity, CMN). It was a pleasure to work with all of you.

On a personal note, I would like to take the opportunity to thank a few exceptionally important people who were instrumental in this achievement.

To my parents, as scientists yourselves, you taught me early on about the wonder of nature and the importance of hard work. Considering my elementary school projects included ditch water protozoa microscopy and purple cabbage pH indicators, was there any chance I wouldn't follow in your footsteps? I am so grateful I did. I thank you, along with my brother, Lukas, for unwavering support, guidance and love.

To my husband, from weigh boats to proof-reading, you have been by my side, helping me believe in myself and offering plates of food with hugs or words of encouragement. Without you, I would not have had the courage to go back to school and undoubtedly, I would not have been able to push through the tough times. My deepest thanks are to you, my dear.

To my Finn and my Jay, although being the "beeest mommy" and a "marinithologist" make me proud, the two of you are my greatest pride. I hope I have made you proud too.

Table of Contents

List of Tables

List of Appendix Tables

List of Figures

List of Abbreviations

Abbreviation	Description
AICc	Akaike's information criterion, adjusted for small sample size
AMDE	Atmospheric mercury depletion event
ANOVA	Analysis of variance
BOLD	Barcode of Life Data System
CV	Carnivore
CB	Cape Bathurst
CBS	Canadian Beaufort Sea
CD	Central disk
DF	Deposit feeder
DNA	Deoxyribonucleic acid
DW	Dry weight
FA	Fatty acid
FABM	Fatty acid biomarker
GEM	Gaseous elemental mercury
Hg	Mercury
HSD	Honestly significant difference
MeHg	Methylmercury (CH_3-Hg^+)
MT	Mackenzie Trough
NCBI	National Center for Biotechnology Information
NWRC	National Wildlife Research Centre
POM	Particulate organic matter
PC1	Principal component 1
PC2	Principal component 2
PCA	Principal component analysis
RSD	Relative standard deviation
SD	Standard deviation
SE	Standard error
SI	Stable isotopes
SF	Suspension feeder
TFA	Total fatty acids
THg	Total mercury
TP	Trophic position
VM	Viscera and muscle
WB	Whole body
$\delta^{13}C$	Carbon stable isotope ratio
$\delta^{15}N$	Nitrogen stable isotope ratio
$\delta^{34}S$	Sulfur stable isotope ratio

Chapter 1

General Introduction

Mercury as a contaminant

Mercury (Hg) contamination is a global threat to wildlife and humans (World Health Organization, 2017; United Nations Environmental Programme (UNEP), 2018). Anthropogenic industrial activities, such as coal burning, mining and hydroelectric damming, have increased Hg concentrations worldwide to nearly five times that which would occur naturally and account for approximately 90% of the Hg burden in animals in the Arctic (Dietz et al., 2009; AMAP, 2011; UNEP, 2018). The organic form of mercury, methylmercury (MeHg), is of most concern owing to its ability to biomagnify through food webs (Morel et al., 1998). The toxicological effects of MeHg were first documented in the mid 1800's (Edwards, 1865). Since then, a suite of neurological, immunological, physiological, genetic, developmental and reproductive dysfunctions have been associated with exposure to MeHg (National Research Council, 2000; Scheuhammer et al., 2012; Chételat et al., 2020). The methylation of mercury occurs predominantly in aquatic environments, exposing aquatic animals to higher concentrations of MeHg than terrestrial animals (Fitzgerald et al., 2007; UNEP, 2018).

Within aquatic environments, the greatest increase in MeHg accumulation occurs when primary producers, such as diatoms, dinoflagellates and cyanobacteria, passively absorb MeHg from the ambient water (Lee and Fisher, 2016). Methylmercury then enters marine food webs when these algae and bacteria are eaten by zooplankton, suspension feeders and deposit feeders and secondarily by carnivores and scavengers (Atwell et al., 1998; Braune et al., 2015). Methylmercury bioaccumulates in organisms over time and biomagnifies as it is transferred between trophic levels (Lehnherr, 2014). The degree to which MeHg bioaccumulates varies by location with marine life in the Canadian Beaufort

Sea (CBS) consistently containing higher amounts of Hg and MeHg than other Arctic locations (Brown et al., 2016; Pomerleau et al., 2016; St. Louis et al., 2017). The reasons for spatial variation of Hg accumulation are due a number of unique environmental processes that occur in the Arctic Ocean as well food web processes that influence dietary exposure in biota (AMAP 2011; Córdoba-Tovar et al., 2022).

Mercury in the Arctic Ocean

Diverse habitats, polar seasonality and the variety of ways Hg can enter and leave the system make Hg dynamics in the Arctic Ocean complex (Braune et al., 2015). Oceanic, fluvial and atmospheric transport deliver Hg to the Arctic Ocean (Kirk et al., 2012; AMAP, 2021). Gaseous elemental mercury (GEM) has a long residence time in the atmosphere and enters the Arctic from across the globe via long-range atmospheric transport (Steffen et al., 2015; Tang et al., 2020). At polar sunrise, atmospheric mercury depletion events (AMDE) occur in which GEM is rapidly converted to reactive gas phase mercury via photochemically-initiated reactions and deposited onto Arctic ice and snow (Steffen et al., 2008). Once deposited, Hg either remains settled or is chemically reduced back into GEM and re-emitted into the atmosphere (Steffen et al., 2015). The spring freshet following ADME and polar sunrise acts as a conduit for deposited Hg to enter streams and rivers (Leitch et al., 2007). Upwards of 80,000-108,000 kg of Hg is estimated to be delivered per year to the Arctic Ocean during this influx of pan-Arctic river water (Fisher et al., 2012; Kirk et al., 2012). Coastal erosion is the second largest contributor to Arctic Ocean Hg, allowing the Hg sequestered within soils to enter the marine environment (Stern et al., 2012). As the Arctic Ocean is semi-enclosed by land, there is restricted exchange with Pacific and Atlantic water masses however both these oceans are

sources of Hg (Outridge et al., 2008). The most recent Hg mass balance estimates that long-range atmospheric transport, riverine influx, meltwater, coastal erosion and oceanic inputs account for 179,000 kg of Hg delivered to the Arctic Ocean annually (Soerensen et al., 2016). These environmental processes generally result in inorganic Hg being the most abundant form of Hg in seawater yet Fitzgerald et al. (2007) reported MeHg as the dominant form (>80 % THg) in upper trophic level animals within marine environments.

Though the methylation of Hg can occur abiotically, the formation of MeHg occurs primarily through biotic processes (Celo et al., 2006). Biotic methylation takes place in the marine water column, carried out by primary producers and heterotrophic bacteria, and in anaerobic sediment by sulphate-reducing bacteria (Compeau and Bartha, 1985; Lehnherr, 2014). Wang et al. (2012) found that while sediment-derived MeHg was a contributor to Arctic Ocean MeHg, water column methylation processes may deliver the bulk of MeHg to marine environments. Methylation rates are influenced by the bioavailability of Hg and dissolved organic matter, microbial activity, oxygen levels, pH and temperature within the water column (Ullrich et al., 2001; Celo et al., 2006; Wang et al., 2012; Lehnherr, 2014).

Once Hg is converted to the more bioavailable form, MeHg, it is taken up by bacteria and phytoplankton which are primary energy sources that support Arctic Ocean food webs (Mason et al., 1996; Bourgeois et al., 2017). There are differences in the rates of MeHg accumulation among primary producers generally due to differences in cellular surface area-to-volume ratios (Lee and Fisher, 2016). Variation in MeHg concentrations at the base of the food web can be reflected in the rates of MeHg transferred to higher

trophic levels (Pomerleau et al., 2016). Identifying correlations between energy sources and MeHg concentration can illuminate dietary MeHg exposure pathways (Chételat et al., 2020). Diet characterization of invertebrates based on specific dietary indicators, trophic position and feeding guild, are outlined in the following section.

Dietary indicators of MeHg uptake

The use of dietary indicators, also known as food-web tracers, hinges on the principal that biochemical signatures of consumers reflect those found in their diet (Parzanini et al., 2019). Dietary MeHg exposure is commonly investigated through dietary indicators such as stable isotope ratios and fatty acid signatures (Chételat et al., 2020). Carbon, nitrogen and sulfur occur in nature as different isotopes with varying numbers of neutrons within their atomic nuclei (Fry, 2006). Biological processes are known to fractionate isotopes in consistent manners creating isotope ratios that can be used to indicate food sources and food web dynamics (Petersen and Fry, 1987). Stable carbon, nitrogen and sulfur isotope ratios are reported using delta notation (δ), expressed as per mil (‰) and are calculations using the formula:

$$\delta X\ (‰) = \left[\frac{(R\ \text{sample} - R\ \text{standard})}{R\ \text{standard}} - 1\right] \times 1000$$

where X represents ^{13}C, ^{15}N or ^{34}S and R is the corresponding ratio of $^{13}C/^{12}C$, $^{15}N/^{14}N$ or $^{34}S/^{32}S$.

The positive relationship between animal nitrogen stable isotope values ($\delta^{15}N$) and MeHg concentrations is well established and has been widely used to study contaminant biomagnification (Atwell et al., 1998; Lavoie et al., 2010; Fox et al., 2014;

Góngora et al., 2018). The $\delta^{15}N$ value of prey is enriched in the consumer at a rate of 3.4 ‰ per trophic level and provide a metric for determining trophic position within food webs (Post et al., 2002). In marine food webs, baseline $\delta^{15}N$ values vary spatially due to environmental factors such as salinity, depth and temperature (Stasko et al., 2018). Baseline $\delta^{15}N$ values can also vary temporally with seasonal fluctuations in abundance of primary producers (Jennings and Warr, 2003).

Using carbon stable isotope ratios ($\delta^{13}C$) to elucidate animal habitat use provides a tracer of environmental availability and uptake of MeHg (Elliot and Elliot, 2016; Chételat et al., 2020). The $\delta^{13}C$ values of consumers reflect the $\delta^{13}C$ values of their diet with a minor enrichment rate of approximately 0.4 ‰ per trophic level (DeNiro and Epstein, 1978; Post, 2002). In marine systems, lower $\delta^{13}C$ values indicate dependence on benthic or terrestrial resources whereas higher $\delta^{13}C$ values reflect a more marine or pelagic food supply (Coelho et al., 2013). Stable carbon isotopes vary spatially in the Arctic Ocean, depending on oceanographic currents and freshwater input (Schell et al., 1998; Pomerleau et al., 2016). Tissue type (e.g., whole body, muscle) and lipid content can influence $\delta^{13}C$ signatures necessitating, in some cases, acidification to remove carbonates followed by lipid-extraction, or mathematical lipid normalization to facilitate intra- and interspecific comparisons (Jacob et al., 2005; Bodin et al., 2007).

Similar to $\delta^{13}C$, sulfur stable isotope ratios, denoted as $\delta^{34}S$, indicate foraging habits and can identify situations where habitat use leads to increased exposure to MeHg (Chételat et al., 2020). Sulfur stable isotopes values can be particularly useful in food web

studies because, unlike carbon and nitrogen stable isotopes, they do not fractionate during transfer through food webs (Elliot and Elliot, 2016). Marine species that live in the water column have higher $\delta^{34}S$ values, close to the $\delta^{34}S$ of open ocean water (~21 ‰; Tostevin et al., 2014) while benthic species living in close proximity to sulfate-reducing bacteria in sediment, tend to have lower $\delta^{34}S$ values (Connolly et al., 2004; Fry et al., 2011). Spatial variation of $\delta^{34}S$ values in estuaries allows for differentiating resource uptake between freshwater influence (lower $\delta^{34}S$ values) and marine influence (higher $\delta^{34}S$ values) and can therefore be used to examine uptake pathways of Hg (Peterson and Fry, 1987; Willacker et al., 2017).

Similar to stable isotopes, fatty acid profiles can be used to characterize diet (Hebert et al., 2006). Fatty acids are hydrophobic molecules found in all organisms that play crucial roles in cellular and physiological functions (Graeve et al., 1997). Essential FAs are principally produced de novo in primary producers (Kelly and Scheibling, 2012; Parzanini et al., 2019). Due to variations in carbon chain length as well as the number and location of double bonds, FA nomenclature has been standardized as A:Bn-X, where A indicates the number of carbon atoms, B indicates the number of double bonds between carbon atoms and X indicates the location of the first double bond in relation to the methyl group at the beginning of the FA molecule (Budge et al., 2006). For example, docosapentaenoic acid (DPA, C22:5n3) has 22 carbon atoms with 5 double bonds, the first of which is located at the third carbon from the terminal methyl group.

Fatty acid analysis is a useful method to illustrate dietary resources because bacteria, copepods and primary producers, such as diatoms and dinoflagellates, have unique FA signatures that when consumed, are often carried unmodified through the food web, sometimes in an accumulative manner (Budge et al., 2006). Further details of specific FA and FABMS as dietary signatures can be found in Dalsgaard et al. (2003), Budge et al. (2006), and Kelly and Scheibling (2012). In benthic invertebrates, FAs and FABMs can assist with identifying geographical differences of food sources, preferential feeding zones, trophic relationships and benthic-pelagic interconnectivity (Graeve et al., 1997; Parrish et al., 2000; Stowasser et al., 2009; Hebert and Popp, 2018).

Methylmercury in benthic invertebrates

The benthic invertebrate community of the CBS is abundant and diverse, representing all categories of consumers, including herbivorous suspension feeders, deposit feeders scavengers and carnivores (Conlan et al., 2008; Macdonald et al., 2010). Due to their relatively small habitat range, benthic invertebrates are useful indicators of local MeHg bioavailability (Bilyard, 1987). Methylmercury uptake in benthic organisms can occur *in-situ*, directly from the bulk sediments and porewater or by feeding on pelagic organic material as it settles out from the water column onto the benthic boundary layer (Piepenburg et al., 1997; Chen et al., 2008). Benthic invertebrate SI and FA reflect spatial variation in primary production and inputs of organic matter that reaches the benthos (Morata et al., 2008). The organic matter that reaches the ocean floor is comprised of terrestrial matter, pelagic and sympagic plankton and phytodetritus, along with pelagic animal carcasses and local macroalgae (Kelly and Scheibling, 2012; Yunda-Guarin et al., 2021). Combining FA and SI dietary tracers may be useful to evaluate complex food web

dynamics and multiple MeHg exposure pathways, across a wide variety of taxa (Dalsgaard et al., 2003; Marziali et al., 2021).

Loria et al. (2020) recently outlined the necessity for studies to contribute to the knowledge gap in baseline concentrations of MeHg in Arctic benthic fauna. It is common for studies involving benthic invertebrates to only focus on a few species and their MeHg concentrations within the scope of MeHg biomagnification (e.g., Clayden et al., 2015; Rigét et al., 2007). Loseto et al. (2008) and McMeans et al. (2015) however included a wider variety of benthic invertebrates along with benthic fish in their biomagnification studies. Animals that forage benthically have been shown to have higher Hg concentrations than those using pelagic food sources (Cossa and Gobeil, 2000; Eagles-Smith et al., 2008; Loseto et al., 2008).

Study overview

The main objective of this study was to investigate relationships between trophic level, dietary indicators and MeHg concentrations in benthic invertebrates of the CBS. Nitrogen, carbon and sulfur stable isotope signatures were evaluated for their ability to explain MeHg concentrations, as were individual FAs and FABMs. In addition, due to the paucity of ecological data available for Arctic benthic invertebrates, correlations among dietary indicators were also examined to expand our understanding of their diet. In efforts to best determine the drivers of MeHg bioaccumulation, all dietary indicators were included in statistical model development with the goal of finding a subset of the variables that explained the highest percent of MeHg concentrations in the study invertebrates.

This study presents the most comprehensive dataset of MeHg concentrations in Arctic benthic marine invertebrates, supported by both traditional and modern taxonomic methods. The assessment of MeHg uptake pathways was improved by the inclusion of DNA barcoding to distinguish between cryptic taxa as well as the inclusion of species-specific ecological traits. This study generated valuable baseline information on food web structure and MeHg concentrations, which can be used to track long-term changes in this ecosystem.

Chapter 2

Trophic position, diet and location influence methylmercury concentrations in benthic invertebrates of the Arctic Ocean

Abstract

This study investigated drivers of methylmercury (MeHg) concentrations in Arctic benthic invertebrates of the Canadian Beaufort Sea. A combination of carbon, nitrogen and sulfur stable isotopes and fatty acid analysis were used to examine the influence of trophic position and diet on MeHg concentrations in 476 individuals from 51 species of benthic invertebrates from three different feeding guilds. Individuals were assigned to species (n = 30) or higher taxonomic level (n = 21) based on DNA-barcoding along with traditional taxonomy. Biomagnification patterns were characterized across the faunal assemblage with a range in MeHg concentrations from 3 to 421 ng/g (dry weight basis) over three trophic positions ($\delta^{15}N$ range 4.4-14.2 ‰). Multivariate models indicate that within the benthic food web, energy sources had small but significant effects on MeHg bioaccumulation. Carbon stable isotopes were weakly correlated to MeHg concentrations for a subset of samples, suggesting terrestrial and benthic energy sources contributed to slightly higher MeHg burdens. Sulfur isotopes were unrelated to MeHg concentrations. Fatty acid analysis revealed that reliance on diatom and aquatic resources resulted in lower MeHg concentrations. Conversely, reliance on dinoflagellate and benthic resources resulted in higher MeHg concentrations. When trophic position and diet were accounted for, site-specific differences in MeHg were observed; specifically, higher MeHg concentrations at a site closer to the Mackenzie River mouth. Although the reasons for this spatial variation remain undetermined, this study suggests that localized exposure accounts for significant variation in MeHg concentrations.

Introduction

Little research has been conducted on benthic invertebrate MeHg concentrations and exposure pathways in benthic food webs of the Arctic Ocean despite MeHg being a widely known neurotoxicant with biomagnifying properties. This knowledge gap presents a significant hole in the understanding of marine food web MeHg dynamics (Loria et al., 2020). Benthic fauna live within (infauna) or upon (epifauna) sediment and are in contact with bottom water and sediment, a zone shown to have high concentrations of MeHg and where inorganic Hg is actively methylated (St. Louis et al., 2017; Cossa and Gobeil, 1999). Benthic invertebrates are preyed upon by arctic cod (Majewski et al., 2017), sharks (McMeans et al., 2015), seals (Wang et al., 2016), diving sea birds, walruses, grey whales (Lovvorn et al., 2018) and beluga whales (Loseto et al., 2008). Thus, benthic animals are a conduit for energy and nutrient transfer from the sediment and benthic boundary layer to the pelagic food web in the water column above (Chen et al., 2008; Griffiths et al., 2017). These dietary pathways also introduce benthic MeHg to the entire Arctic Ocean food web (Lehnherr, 2014; Harding et al., 2018).

Methylmercury is primarily absorbed through diet, therefore understanding dietary pathways within food webs allows for characterization of MeHg sources (Hebert et al. 2006; Chételat et al., 2020). Dietary pathways are investigated using trophic position and feeding guild comparisons made possible by comparing carbon, nitrogen and sulfur stable isotopes (SI) along with FA and FABM signatures (Lavoie et al., 2013; McMeans et al., 2015; Elliot and Elliot, 2016, see Table 2.1). Trophic position (TP) is a major driver of MeHg biomagnification in marine food webs (Lavoie et al., 2013). Trophic position is estimated using stable nitrogen isotope ($\delta^{15}N$) because the ^{15}N isotope

enriches at a consistent rate of approximately 3.4 ‰ per TP (Minagawa and Wada, 1984; Post, 2002). The source of the organic matter in invertebrate diets is also considered an important influence in contaminant uptake pathways (Lavoie et al., 2010). Sulfur SI ratios ($\delta^{34}S$) in marine animals do not fractionate during trophic transfer and are influenced by proximity or consumption of prey that inhabit sulfate-reducing environments such as anoxic sediments (Petersen and Fry, 1987). Lower $\delta^{34}S$ signatures therefore indicate benthic over pelagic foraging, however lower $\delta^{34}S$ values can also reflect freshwater or terrestrial energy sources rather those of oceanic origin (Habicht et al., 1998; Hobson, 1999; Hebert et al., 2008, Chételat et al., 2020). To offset the potential ambiguity of $\delta^{34}S$ indications, it is useful to consider $\delta^{34}S$ values in conjunction with stable carbon isotope ratios ($\delta^{13}C$) values. Values of $\delta^{13}C$ enrich minimally through food webs (0.4 ‰ per trophic level) thus reflect those of the food web primary producers (Hecky and Hesslein, 1995; Post, 2002). Higher $\delta^{13}C$ values indicate reliance on marine/pelagic resources and mid-range $\delta^{13}C$ values reflect a more terrestrial food supply while the lowest $\delta^{13}C$ indicate reliance on freshwater carbon sources (Middelburg and Herman, 2007; Coelho et al., 2013).

Similar to stable isotopes, FA and FABM reveal predator-prey relationships, primary energy sources and foraging behavior (or feeding guild) due to their conservative transfer through food webs (Graeve et al., 1997; Dalsgaard et al., 2003; Iverson et al., 2004). Combining SI and FA/FABM signatures provides the means of cross-validating natural history feeding guild information (e.g., deposit feeder, suspension feeder and carnivore), detailing connections within food webs and understanding which dietary

sources are significantly contributing to Hg bioaccumulation (Petersen and Fry, 1987; McMeans et al., 2015; Chételat et al., 2020).

Table 2.1. Summary of study dietary indicators and uses in determing food web dynamics and resource use (references given in text and Table 2.2).

Indicator	Trophic Position	Energy Resources	Foraging Location
Stable Isotopes	$\delta^{15}N \uparrow$ 3.4 ‰ per trophic level	Higher $\delta^{13}C \rightarrow$ Marine-origin Lower $\delta^{13}C \rightarrow$ Freshwater-origin Higher $\delta^{34}S \rightarrow$ Marine-origin Lower $\delta^{34}S \rightarrow$ Terrestrial-origin	Higher $\delta^{13}C \rightarrow$ Benthic Lower $\delta^{13}C \rightarrow$ Pelagic Higher $\delta^{34}S \rightarrow$ Pelagic Lower $\delta^{34}S \rightarrow$ Benthic
Fatty Acid	Carnivory C16:0 C18:1n9c C20:1n9	Diatom C14:0, C16:1n7, C20:5n3 Dinoflagellate C18:0, C22:5n3, C22:6n3	Benthic C20:4n6
Fatty Acid Biomarkers	Copepod FABM	Aquatic FABM Terrestrial FABM Bacteria FABM Dinoflagellate FABM Diatom FABM	Pelagic Aquatic FABM Benthic Terrestrial FABM

A suite of factors predispose the Arctic Ocean and its inhabitants to higher concentrations of Hg (Douglas, 2012). Long-range atmospheric transport, riverine output, coastal erosion and oceanic pathways carry predominantly inorganic Hg to the Arctic Ocean where Hg can accumulate due to the Arctic Ocean being semi-isolated (AMAP, 2011). Once in the aquatic environment Hg is methylated in sediments as mentioned, but also in the water column through microbial and phytochemical pathways to form MeHg (Macdonald and Loseto, 2010; Lehnherr et al., 2011). Methylmercury is efficiently assimilated through diet and can bioaccumulate and biomagnify through food webs (Braune et al. 2015). Lehnherr et al. (2014) suggested that in Arctic aquatic dietary pathways, MeHg concentrations between water and fish can biomagnify more than one million times, putting top predators and humans at risk. This is important because MeHg accumulation can cause neurological, immunological, physiological, genetic, developmental and reproductive effects in vertebrates at high levels of exposure (National Research Council et al., 2000; Scheuhammer et al., 2012; Evers, 2018).

Spatial and temporal trends in MeHg accumulation have been well documented in Arctic megafauna such as beluga (Loseto et al, 2008), polar bears (Routti et al., 2011) and seals (Brown et al., 2016). Trends also have been reported for fish (Stern et al., 2005) and plankton (Pomerleau et al., 2016). By comparison, MeHg profiles in benthic invertebrates have received minimal research focus (Loria et al., 2020). The objective of this study was to examine and identify factors that influence MeHg bioaccumulation in Arctic marine benthic invertebrates. This study examined whether invertebrates living in proximity to the Mackenzie River exhibit higher concentrations of MeHg than individuals of the same

species collected further from the influence of the Mackenzie, at Cape Bathurst. In addition to spatial differences, I predicted that the well-established process of biomagnification, inferred from nitrogen stable isotope estimates of trophic position, is a dominant driver of MeHg concentrations even within the trophic range represented by the benthic invertebrate faunal assemblage. I also investigated whether values of $\delta^{13}C$, $\delta^{34}S$, and FA and FABM compositions correlate with MeHg concentrations in CBS benthic invertebrates. This study generated a comprehensive dataset of MeHg in Arctic benthic marine invertebrates, supported by the use of DNA barcoding for species identification and diet characterization using multiple dietary tracer analyses. Given the role that benthic organisms play in MeHg transfer to the rest of the marine food web, this study should advance the understanding of MeHg accumulation trends in the CBS.

Methods

Study area

The Canadian Beaufort Sea is located in the western Canadian Arctic Ocean, north of the Yukon, Northwest Territories and Nunavut. Its deepest point is in the northern Canada Basin while the southern extent is characterized by a large, shallow continental shelf approximately 120 km wide by 530 km long (Carmack and MacDonald, 2002). This study took place at two locations on the CBS shelf during the summer of 2007. Benthic invertebrate assemblages were collected at the northwestern tip of Cape Bathurst (CB, 22 m water depth, mean coordinates of trawl, 70.69522°, -128.83926°) and off the eastern coast of Herschel Island in the Mackenzie Trough (MT, 116 m water depth, mean coordinates of trawl 69.61249, -138.56257) (Figure 2.1). Both locations experience periodic wind-driven, topographically-enhanced upwelling events in which

nutrient-rich water flows up the shelf break from deeper waters to the north (Carmack and Kulikov, 1998; Williams and Carmack, 2008). As a result of their nutrient rich habitat, fauna in both locations were diverse and abundant thereby permitting collection of invertebrates from a wide variety of taxa (Conlan et al., 2013).

Across the shelf and the shelf break, four water masses are bathymetrically separated by temperature and salinity (Lansard et al., 2012). Nearshore and across the surface of the CBS (0-60 m) is a mix of marine and fresh water from the sea ice melt and river influx. Below the mixed layer is the Pacific water mass (cold, low salinity, 60-200 m) followed by the Atlantic water mass (warmer, higher salinity, 300-900 m). The coldest and most saline Arctic Ocean water mass is found beyond 900 m depth (Majewski et al., 2017). The CB site, which has a depth of 22 m, is found in the mixed water layer however due to the upwelling nature of the site, it is exposed to marine water masses (Williams and Carmack, 2008). The MT site, at a depth of 116 m, is found in the Pacific water mass yet, is seasonally exposed to greater freshwater input due to its proximity to the Mackenzie River delta (Carmack and Macdonald, 2002).

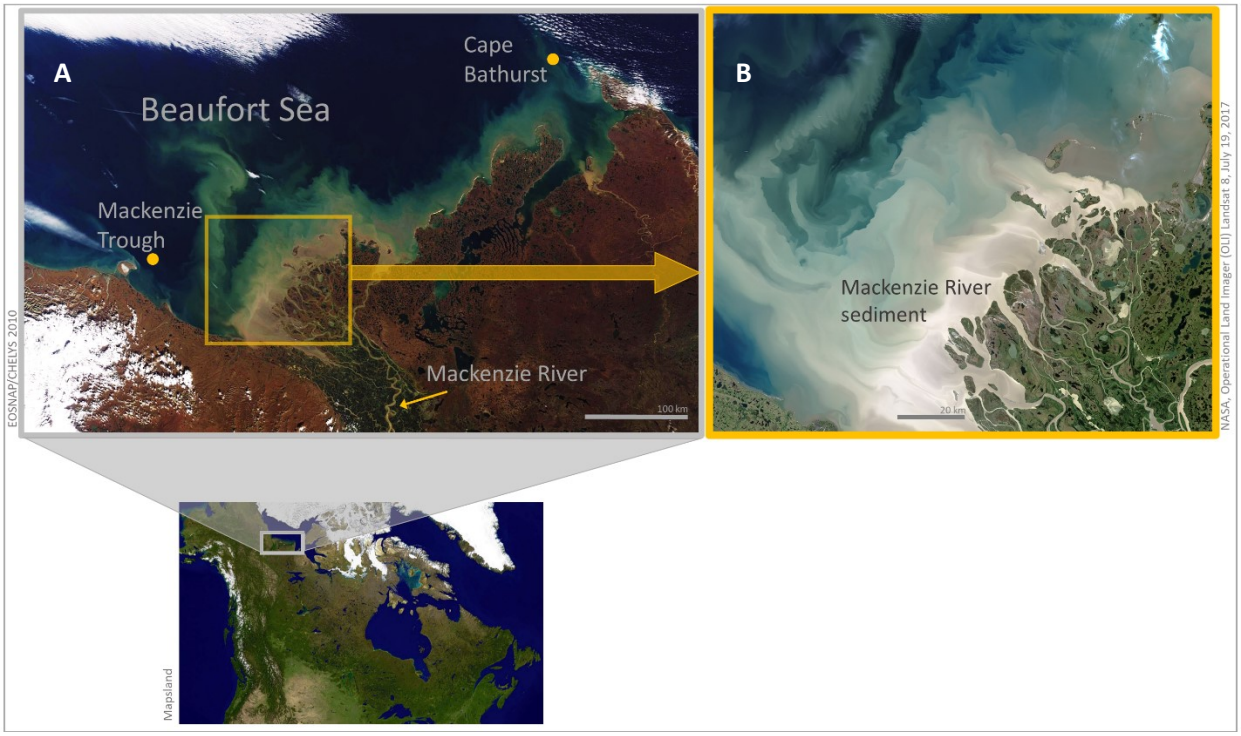

Figure 2.1. Map of Canada with insets of A) Canadian Beaufort Sea with study sites (yellow points) and B) Mackenzie River sediment plume (yellow rectangle).

Field collection

In collaboration with the Department of Fisheries and Oceans Canada, marine invertebrates were collected on July 31 and August 2, 2007 from two sites on the Mackenzie shelf of the CBS. While aboard the Canadian Coast Guard Ship Nahidik, a 3 m wide benthic beam trawl was deployed to the ocean floor for approximately 20 minutes at an average speed of ~1 m/s (Majewski et al., 2009). Animals were collected from an area of approximately 3600 m^2 of the seafloor (see Figure 2.2). The trawl's net and the cod-end consisted of 3.17 cm stretched nylon mesh, with the cod-end itself lined with 0.63 cm nylon mesh (Majewski et al., 2011). An effort was made to select the same species from both locations to allow for paired comparisons between locations. Animals were depurated in salt water for 24 hours before being frozen aboard the ship under nitrogen atmosphere at -80°C. Samples were shipped on dry ice to the Canadian Museum of Nature and stored long-term at -80°C.

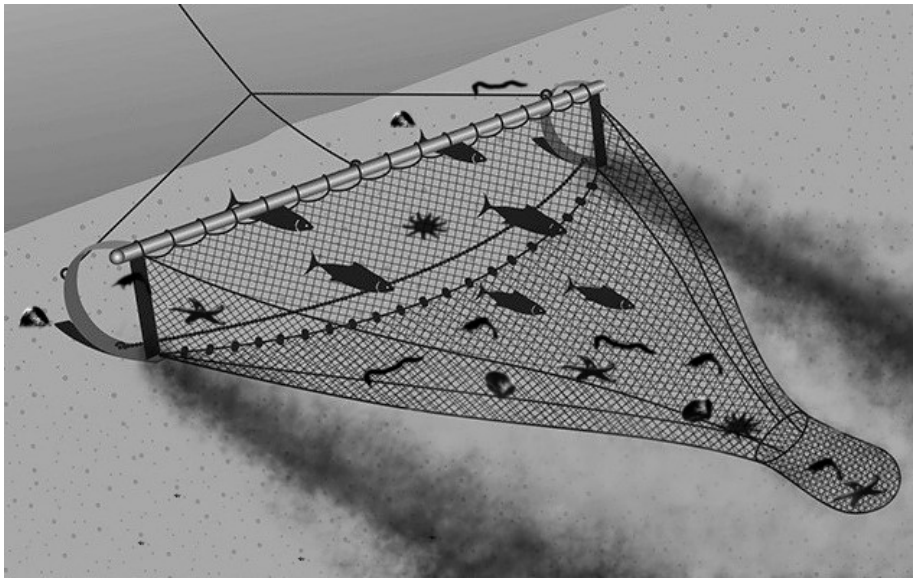

Figure 2.2. An illustration of fauna collection using a benthic beam trawl. Modified and reprinted with the permission of www.sea-trawl.com.

DNA sequencing

Prior to homogenization, a small amount of tissue was taken from species voucher specimens for DNA barcoding analysis. DNA sequencing was performed at the Canadian Museum of Nature's Natural Heritage Campus (Gatineau, Canada) following an adapted version of the method found in Ivanova et al. (2006). Lobo primers were used to amplifiy of the 5' end of the mitochondrial gene cytochrome *c* oxidase subunit I, the mitochondrial DNA region widely used as the unique identifier of animal species (COI-5P, Lobo et al., 2013). Sequencing was conducted on an Applied Biosystems 3500xl Genetic Analyzer. Forward and backward COI-5P sequences were combined using Geneious software, version 7.0.6. Generated sequences were queried for alignment matches within the Barcode of Life Data System v4 (BOLD) and National Center for Biotechnology Information (NCBI) sequence reference libraries. Invertebrates were identified using a combination of DNA barcode alignment best matches and field identifications with the exception of most amphipod, shrimp and polychaete species, which were identified primarily based on DNA barcode matches. In situations where one specimen matched multiple species within the same genus to a similar extent, only the genus was retained with "sp." used to indicate unknown species. The same nomenclature was applied for barcode queries that returned higher order taxonomic matches (i.e., phylum, class, order, and family). For specimens whose DNA was not amplified successfully and those whose barcodes were inconclusive, the field identification to the lowest taxonomic level was used. Once the invertebrate taxa were confirmed they were grouped into feeding guilds based on previously published literature (See Appendix I). Based on previously published studies, taxa were separated by feeding guilds, broadly categorized as suspension feeders (SF) which filter food from the water at the benthic boundary layer, deposit feeders (DF)

which feed on sediment and pelagic particles that have settled thereon, and carnivores (including scavengers, CV) which feed on benthic and epibenthic fauna as well as carcasses of pelagic animals that have settled to the seafloor.

Tissue preparation for chemical analysis

An assortment of homogenization techniques were employed because of the diversity of body structures of the invertebrates in this study. If present, eggs and juveniles in pericarid crustacean brood pouches were removed prior to homogenization. For bivalves, gastropods and sea stars, muscle and internal viscera were dissected, freeze-dried and homogenized with acid-washed glass mortars and pestles. Cumaceans, amphipods, small isopods, small pycnogonids, sea anemones, corals, sea cucumbers, nudibranchs, nemerteans, polychaetes and sipunculids were freeze-dried whole and homogenized using acid-washed glass mortars and pestles. Larger arthropods, specifically the shrimp and larger isopods and pycnogonids, were homogenized whole using a Retsch MM301 Ball Mill (30 rev/s for 30 s) then freeze-dried. In all cases, invertebrates were freeze-dried for a minimum of 48 hours.

Three shrimp (*Sabinea septimcarinata*) and three isopods (*Saduria sabini*) were dissected to enable tissue-specific analysis of MeHg concentrations. Animals were halved longitudinally; one half was further dissected to isolate exoskeleton from internal muscle and viscera. The exoskeleton and half-body samples were homogenized via ball mill then freeze-dried. Muscle and viscera samples were freeze-dried then homogenized using acid-washed glass mortars and pestles.

Composite samples for chemical analyses were created by combining subsamples of individuals of the same species from the same location. Two sets of composite samples were created from the same set of individuals: one set for fatty acid analysis (n = 64) and one set for MeHg analysis (n = 147) and analysis of carbon, nitrogen and sulfur stable isotopes (n = 71, 147, and 145, respectively).

Fatty acid analysis

Fatty acid were analyzed at the National Wildlife Research Centre (NWRC, Environment and Climate Change Canada, Ottawa, Canada) following modified methods described by Schlechtriem et al. (2008) and Bligh and Dyer (1959). Briefly, FAs were extracted using a 2:1 chloroform-methanol solution containing 0.01 % butylated hydroxyl toluene, methylated using 1 % methanolic sulfuric acid and quantified on a Hewlett-Packard 6890 GC with the equipped with a flame ionizing device and Supelco SP-2560 column (100 m x 0.25 mm i.d. x 0.20 um thick film). A more detailed version of the method is described in Hebert et al. (2006). Fatty acid peaks in the samples were compared to those of known FA retention times using a 37-component FA standard (Supelco; no 47885-U). Fatty acids were reported proportionally as percent total FA composition (% TFA) for selected FAs. Eight method blanks were conducted throughout the sample analyses; all showed less than 2 mg/g (dry weight (DW)) contamination. A known amount of 5α-cholestane was added to each sample for calibration and recovery calculations. The surrogate 5α-cholestane was used to estimate recovery of all FAs, which was calculated by the GC Chemstation software. Only FAs that constituted greater than 5 % of total FAs in more than one taxon (hereafter referred to as major FAs) were reported. Fatty acid biomarkers were calculated as sums or ratios of FAs, based on

previous use as dietary indicators (Table 2.1). Five duplicate samples were analysed for method precision. The duplicate values for the ten major FAs had a mean relative standard deviation (RSD) of 6.6 % (range = 4.1-11.3 %) while the 28 FAs with very low percent compositions (< 2.7 % TFA) had lower duplicate precision with a mean RSD of 22.4 % (range = 0.0-141.4 %) because the values were closer to the detection limits of the GC-FID. To assess the FA method accuracy, an internal standard sample of Herring Gull egg was analyzed to quantify recoveries of 17 FAs. The average recovery across all 17 detectable FAs was 103 % (n = 5, average recovery range per analyte = 85-126 %).

Stable isotope analysis

Stable isotope analyses were conducted at the Ján Veizer Stable Isotope Laboratory (University of Ottawa, Ottawa, Canada) using a Delta Advantage Isotope Ratio Mass Spectrometer interfaced to a Conflo III and Vario EL Cube elemental analyzer. Stable isotopes were measured on untreated samples. Tin capsules for carbon and nitrogen SI analyses contained 1 ± 0.1 mg of dry tissue while those for sulfur contained 6 ± 0.5 mg. Calculations for $\delta^{13}C$, $\delta^{15}N$ and $\delta^{34}S$ calculations were based on the standard reference materials Vienna-PeeDee Belemnite, atmospheric N_2 gas and Vienna-Canyon Diablo Troilite, respectively. Mean standard deviation for duplicate SI samples (n = 14 for each SI ratio) were: $\delta^{13}C$, 0.10 ± 0.06 ‰; $\delta^{15}N$, 0.29 ± 0.43 ‰; and $\delta^{34}S$, 0.44 ± 0.44 ‰. Analytical accuracies using internal reference material samples (glutamic acid for $\delta^{13}C$ and $\delta^{15}N$, n = 6; argentite for $\delta^{34}S$, n = 11) were 100.2 ± 0.2 ‰ for $\delta^{13}C$, 101.3 ± 1.8‰ for $\delta^{15}N$ and 103.3 ± 9.4 for $\delta^{34}S$.

Table 2.2. Major FAs and FABMs used in this study and their dietary sources.

Major FA/FABM	Sources
C14:0 Myristic Acid	Diatom [h]
C16:0 Palmitic Acid	Carnivory [c,d]
C16:1n7 Palmitoleic Acid	Diatom [b]
C18:0 Stearic Acid	Dinoflagellate [b]
C18:1n9c Oleic Acid	Carnivory, related to copepods [d,f]
C20:1n9 Eicosenoic acid	Copepod [a,d]
C20:4n6 Arachidonic Acid (ARA)	Benthic foraging [j]
C20:5n3 Eicosapentaenoic Acid (EPA)	Diatom [b]
C22:5n3 Docosapentaenoic Acid (DPA)	Dinoflagellate [b]
C22:6n3 Docosahexaenoic Acid (DHA)	Dinoflagellate [b,f]
∑Omega 3: ∑Omega 6	Aquatic carbon source [e]
∑(C18:2n-6 + C18:3n3)	Terrestrial carbon source [a,i]
C22:6n-3/C20:5n-3 (DHA/EPA)	Dinoflagellate diet [b,g]
C16:1n-7/C16:0	Diatom diet [b,i]
∑ (C20:1 + C22:1)	Copepod diet [a,c]
∑ (C15:0 + C17:0)	Bacteria diet [d,i]

[a] Connelly et al., 2014; [b] Dalsgaard et al., 2003; [c] Falk-Petersen et al., 1987; [d] Graeve et al., 1997; [e] Hebert and Popp, 2018; [f] Kelly and Scheibling, 2012; [g] Legeżyńska et al., 2014; [h] Leveille et al., 1997; [i] Mohan et al., 2016; [j] Stowasser et al., 2009.

Trophic position was calculated using $\delta^{15}N$ ratios:

$$TL_{species} = \left[\frac{(\delta^{15}N_{species} - \delta^{15}N_{POM})}{\delta^{15}N_{FC}}\right] + 1$$

where $\delta^{15}N_{species}$ is the $\delta^{15}N$ value of the species in question, $\delta^{15}N_{POM}$ is the $\delta^{15}N$ of the corresponding POM collected at the same location as the species in question and the $\delta^{15}N_{FC}$ is the trophic fractionation constant of 3.4 (Vander Zanden & Rasmussen, 2001; Minagawa and Wada 1984) . Site-specific $\delta^{15}N_{POM}$ was provided by Dr. Patricia Ramlal, DFO (unpublished data; surface water sample, collected on the same day as study invertebrates, in the same general area).

Methylmercury analysis

MeHg concentrations in freeze-dried samples were measured at the NWRC. Samples (20-50 mg) were digested with 17.5 % nitric acid at 60°C for 16 hours. Sample extracts of 50 µL were added to ultrapure water with acetate buffer. Samples were ethylated with 30 µL of sodium tetraethyl borate for 30 minutes before analysis on a Tekran 2700 Methyl Mercury Analyzer (gas chromatography cold-vapor atomic fluorescence spectrophotometer) equipped with a 2621M Automatic sample changer. Method blanks, duplicates and standard reference materials were included with every set of extractions. Method precision, given as RSD for duplicate samples, was 1.8 % (range = 0-5.4 %, *n* = 17). Method accuracy, based on the recovery of MeHg in four standard reference materials (NIST 2976 Mussel Tissue, NRC TORT-3 Lobster hepatopancreas, NRC DORM-4 Fish, IAEA-436 Fish Flesh), was 95 % (range = 87-104 % , *n* = 34).

Statistical analyses

Statistical analyses were performed using R, versions 3.6.3 to 4.1.0. Normality was evaluated with Shapiro-Wilks tests and equality of variance between locations was assessed with Levene's tests. Fatty acid, FABM and MeHg concentrations were log-transformed prior to modelling in order to satisfy normality assumptions. Pearson correlations with Holm-Bonferroni corrected *p*-values were used to determine associations between FA/FABM and SI values and MeHg concentration. One- and two-ANOVAs, Tukey's post-hoc honestly significant difference (HSD) tests, and general linear models were used to investigate relationships between the dietary indicators, location, feeding guild, and MeHg concentrations. Due to the number of variables in this study, generally only statistically significant results were reported.

Four data sets were used (due to differences in sample sizes among explanatory variables) to model SI, FA, FABM, location and feeding guild as independent variables and MeHg concentrations as the dependent variable. For the models that include FA/FABM variables, the SI values and MeHg concentrations reflect a mean value for all samples of a given species because there were fewer FA analyses performed than MeHg and SI analyses. The best models for each data set were selected using Akaike's Information Criterion adjusted for small samples (AICc). The models passed assumptions of variance homogeneity and normality of residuals.

Principal Component Analyses (PCA) using log-ratio transformed FA and log-transformed FABM variables were conducted to reduce the dimensionality of the large dataset and allow for visualization of dominant FA/FABM trends as well as correlations

between independent variables. Principal component loadings represent the correlation between independent variables and each principal component. Individual observations were plotted to visualize the relationship between the data points and principal components and independent variables. Assumptions for the PCA were tested via Bartlett test for collinearity, Kaiser-Meyer-Olkin test for sampling adequacy and correlation matrix positivity.

Results

DNA determinations and faunal composition

Field identifications and DNA determinations confirmed the faunal assemblage of 476 animals consisted of 51 identifiable taxa, some of which are shown in Figure 2.3. The barcoding process amplified barcodes in 72 of the 75 specimens with 65 of the DNA barcodes having sufficient amplification to match DNA barcodes found in the BOLD and NCBI DNA libraries. The percent alignment of the matches was variable, as is seen in Table 2.2. Replicate specimens received identical taxonomic matches though alignment percentages varied. A total of 30 species were found at the CB site and 38 species at the MT site, with 16 species found at both sites. Study taxa, their benthic habitat zone and feeding guilds, are presented in Table 2.3.

Table 2.3. Percent alignment of voucher specimens DNA barcodes with DNA barcodes found in NCBI and BOLD barcode libraries, where n represents number.

Alignment match	Voucher specimens (*n*)	Taxa identified (*n*)
100%	28	23*
99.0-99.9%	21	18*
95.0-98.9%	9	8*
<95%	7	5*
No match	7	6*
No DNA barcode available	3	3

* includes replicate vouchers

Table 2.3. List of taxa in this study with number of species collected (*n*), collection locations, benthic zone and feeding guild (reference for feeding guild are found in Appendix I).

Taxon	*n*	Location	Benthic zone[a]	Suspension feeder	Deposit feeder	Carnivore
Amphipoda	8	CB/MT	I/E	x	x	x
Cumacea	1	CB/MT	I/E		x	
Isopoda	4	CB/MT	I/E		x	x
Decapoda	3	CB/MT	E		x	x
Pycnogonidae	1	CB/MT	E			x
Anthozoa	2	CB/MT	E	x		x
Asterozoa	6	CB/MT	E	x	x	x
Holothuroidea	1	MT	I/E	x		
Nemertea	1	CB	E			x
Sipuncula	1	CB/MT	I		x	
Polychaeta	9	CB/MT	I/E		x	x
Bivalvia	7	CB/MT	I/E	x	x	x
Gastropoda	8	MT	I/E	x	x	x
Nudibranchia	1	CB/MT	E			x

[a] Benthic zone: I, infauna; E, epifauna.

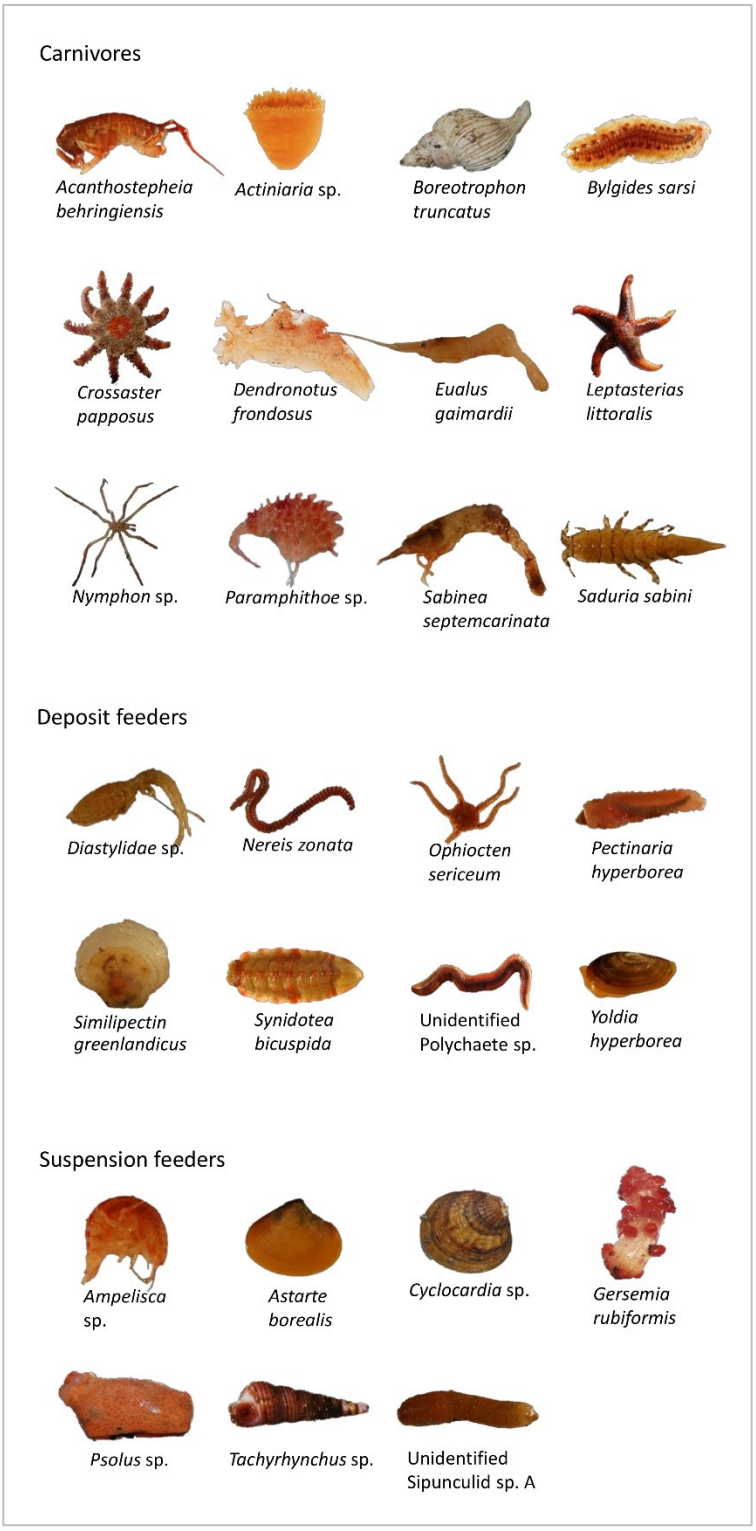

Figure 2.3. Photographs of a selection of species included in this study, organized by feeding guild (animals not to scale, size range 0.5-12 cm). Photo source: C. McClelland.

Methylmercury concentrations

Methylmercury concentrations of individual samples ranged widely from 3 ng/g to 421 ng/g, dry weight. As reported in Table 2.4, the highest mean MeHg concentrations were found at the MT location in the predatory sea star *Crossaster papposus* and the predatory pycnogonid *Nymphonidae* sp. (367 ± 93 ng/g and 299 ng/g, respectively). Meanwhile, the lowest MeHg concentrations were found in the CB amphipods *Ampelisca* sp. and *Arctolembos arcticus* (4 ± 1 ng/g and 7 ± 2 ng/g, respectively). The amphipods and the echinoderms had the greatest intragroup variation in MeHg concentration (7-231 ng/g and 8-367 ng/g, respectively). For the subset of data with the same species present at both locations, both species and the species*location interaction significantly influenced MeHg concentrations (two-way ANOVA, type III, species $p < 0.0001$, species*location $p < 0.0001$, $n = 76$) (Figure 2.4). For the samples used to examine tissue specific concentrations of shrimp and isopod, MeHg concentrations were approximately 2.4 times higher in soft tissues than exoskeleton (ANOVA, $p < 0.05$; Tukey HSD $p < 0.05$, $n = 12$).

Across the whole data set, feeding guild and location significantly influenced MeHg concentrations in the invertebrates (two-way ANOVA, type III, feeding guild $p < 0.005$, location $p < 0.005$, $n = 147$), see Figure 2.5. All feeding guilds showed higher MeHg concentrations at the MT site compared to the CB site (Tukey HSD, $p < 0.005$). When controlling for the influence of location, significant MeHg concentration differences were found within feeding guilds, specifically between deposit feeders and carnivores, and between suspension feeders and carnivores (Tukey HSD, $p < 0.005$ for both).

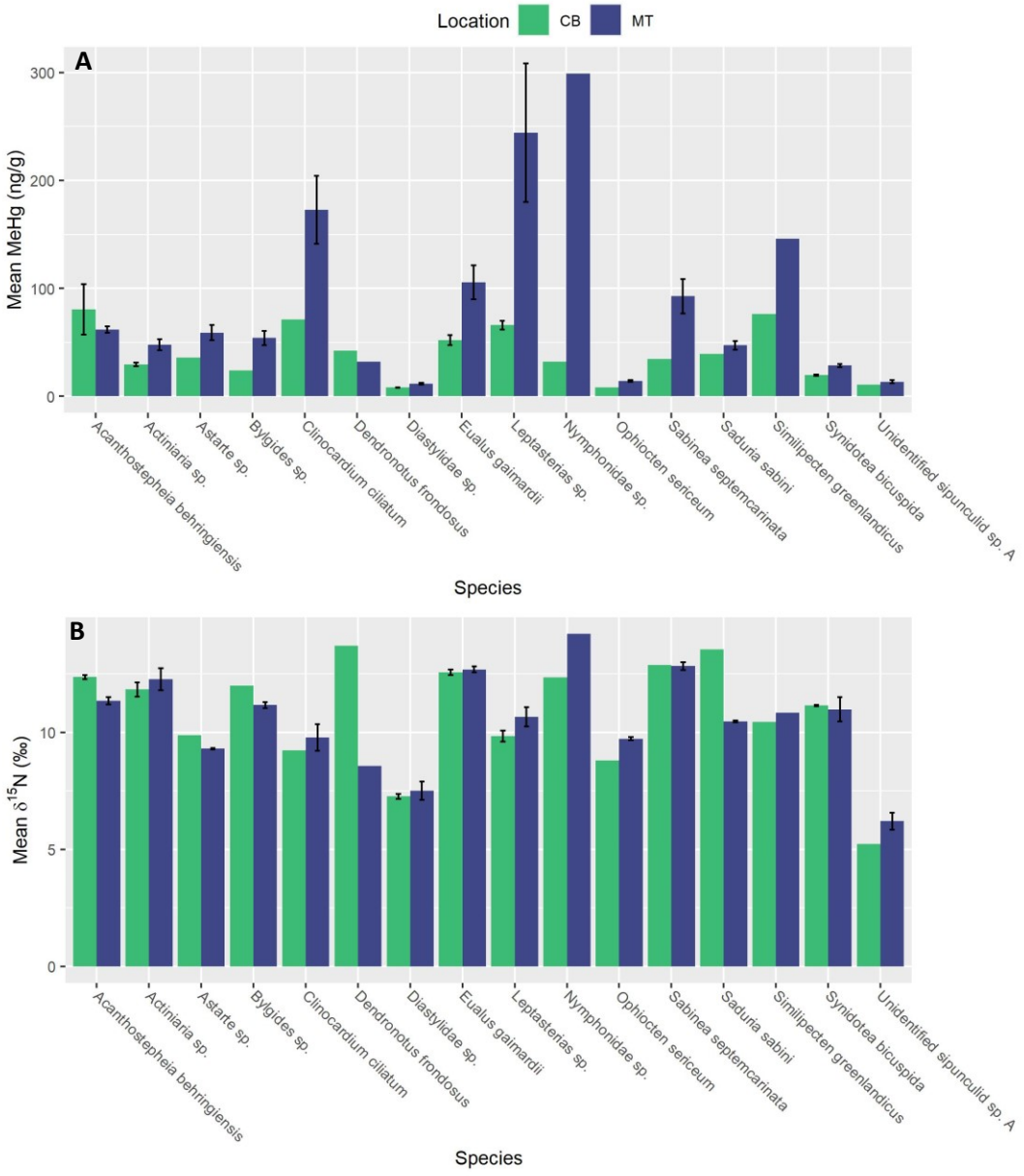

Figure 2.4. Bar graphs (± SE bars) of A) mean MeHg concentrations and B) mean $\delta^{15}N$ values in paired species samples from the Cape Bathurst (CB) and Mackenzie Trough (MT) collection sites.

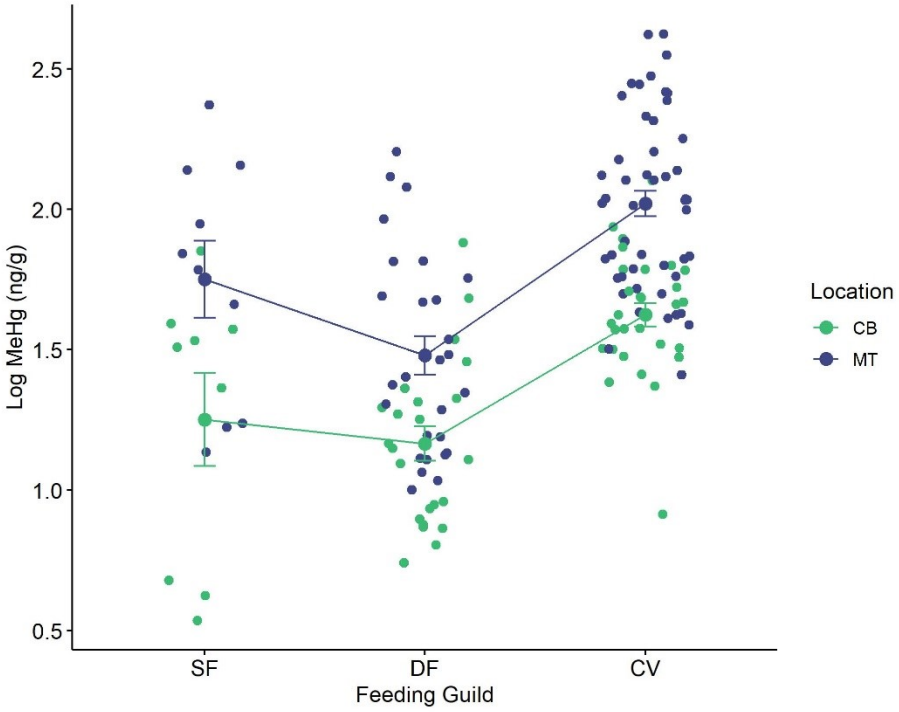

Figure 2.5. Two-factor plot of mean MeHg concentrations (± SE) by feeding guild and location.

Table 2.4. Species, location, feeding guild (FG), tissue, number of individuals (*n* ind) and composites (*n* comp) analyzed for carbon, nitrogen and sulfur stable isotopes and MeHg concentration (± standard deviations) with derived trophic position (TP).

Taxon	Location	FG[a]	Tissue[b]	*n* ind (*n* comp)	$\delta^{15}N$ (‰)	$\delta^{13}C$ (‰)	$\delta^{34}S$ (‰)	MeHg (DW, ng/g)	TP
Amphipoda									
Acanthostepheia behringiensis (L)[c]	CB	CV	WB	7 (3)	12.4 ± 0.2	-	20.6 ± 0.4	80 ± 41	3.5 ± 0
	MT	CV	WB	7 (3)	11.4 ± 0.3	-	18.6 ± 0.4	62 ± 5	3.1 ± 0.1
Acanthostepheia behringiensis (S)[c]	CB	CV	WB	4 (1)	8.6	-	21.1	8	2.2
Ampelisca sp.	CB	SF	WB	12 (3)	7.6 ± 0.6	-	19.7 ± 0.2	4 ± 1	2.1 ± 0.2
Anonyx nugax	MT	CV	WB	10 (3)	13.7 ± 0.5	-	20.7 ± 0.2	231 ± 70	3.7 ± 0.1
Arctolembos arcticus	CB	DF	WB	7 (3)	8 ± 0.7	-	20.5 ± 0.8	7 ± 2	2.2 ± 0.2
Paramphithoe sp.	MT	DF	WB	4 (1)	13.2	-	-	127	3.3
Pleustes panoplus	CB	DF	WB	7 (3)	9.9 ± 0.4	-	21.2 ± 0.9	21 ± 2	2.7 ± 0.1
Rhachotropis aculeata	CB	CV	WB	5 (2)	11.3 ± 0.7	-	20.1 ± 0.2	55 ± 33	3.1 ± 0.2
Unidentified amphipod sp.	MT	CV	WB	7 (3)	12.6 ± 1.3	-	20.6 ± 0.1	79 ± 18	3.4 ± 0.4
Cumacea									
Diastylidae sp.	CB	DF	WB	55 (3)	7.3 ± 0.2	-	21.7 ± 0.2	8 ± 1	2 ± 0.1
	MT	DF	WB	15 (3)	7.5 ± 0.7	-	21.7 ± 0.5	12 ± 1	1.9 ± 0.2
Isopoda									
Munnopsis typica	CB	DF	WB	4 (1)	10.4	-	17	29	2.7
Saduria entomon	MT	CV	WB	7 (3)	11.5 ± 0.2	-	20.8 ± 0.7	53 ± 12	3.1 ± 0.1
Saduria sabini	CB	CV	WB	2 (1)	13.6	-	17.6	39	3.5
	MT	CV	WB	6 (3)	10.5 ± 0.1	-	20.4 ± 0.9	47 ± 7	2.8 ± 0
Synidotea bicuspida	CB	DF	WB	7 (3)	11.1 ± 0.1	-	21.7 ± 0.4	19 ± 1	3.1 ± 0
	MT	DF	WB	7 (3)	11 ± 0.9	-	21.9 ± 0.4	28 ± 3	2.9 ± 0.3
Decapoda									
Eualus gaimardii	CB	CV	WB	10 (3)	12.6 ± 0.2	-	20 ± 0.2	52 ± 8	3.5 ± 0.1
	MT	CV	WB	7 (3)	12.7 ± 0.2	-	20.7 ± 0	106 ± 27	3.4 ± 0.1
Sabinea septemcarinata	CB	DF	WB	3 (1)	12.9	-	20.9	35	3.3
	MT	DF	WB	6 (3)	12.8 ± 0.3	-	17.3 ± 0.4	93 ± 27	3.5 ± 0.1
Spirontocaris sp.	MT	CV	WB	7 (3)	11.3 ± 0.3	-	20.1 ± 1.5	134 ± 26	3 ± 0.1

Taxon	Location	FG[a]	Tissue[b]	*n* ind (*n* comp)	$\delta^{15}N$ (‰)	$\delta^{13}C$ (‰)	$\delta^{34}S$ (‰)	MeHg (DW, ng/g)	TP
Pycnogonidae									
Nymphonidae sp.	CB	CV	WB	18 (1)	12.3	-	20.8	32	3.4
	MT	CV	WB	3 (1)	14.2	-	19.3	299	3.9
Anthozoa									
Actiniaria sp.	CB	CV	WB	9 (3)	11.8 ± 0.5	-22.4 ± 0.4	19.2 ± 0.5	29 ± 3	3.3 ± 0.2
	MT	CV	WB	6 (3)	12.3 ± 0.8	-24.3 ± 0.3	19.6 ± 0.4	48 ± 9	3.3 ± 0.2
Gersemia rubiformis	MT	SF	WB	3 (1)	10.4		23.7	17	2.6
Asterozoa									
Crossaster papposus	MT	CV	VM	8 (3)	12.8 ± 0.2	-21.7 ± 0.8	21.2 ± 0.6	367 ± 93	3.5 ± 0.1
Leptasterias littoralis	CB	CV	VM	6 (3)	9.8 ± 0.4	-21.9 ± 1.1	20.1 ± 0.3	66 ± 7	2.7 ± 0.1
Leptasterias sp.	MT	CV	VM	8 (3)	10.7 ± 0.7	-20.9 ± 0.6	20.5 ± 0.8	244 ± 111	2.9 ± 0.2
Ophiocten sericeum	CB	DF	CD	9 (2)	8.8 ± 0.4	-	22 ± 0.7	8.± 1	2.4 ± 0.1
	MT	DF	CD	14 (3)	9.7 ± 0.1	-	21.8 ± 0.9	14 ± 1	2.6 ± 0
Ophiacantha bidentata	MT	DF	CD	5 (2)	12.4 ± 0.5	-	23.2 ± 0.1	42 ± 10	3.4 ± 0.1
Stegophiura nodosa	CB	DF	CD	7 (2)	10 ± 0.6	-	26.8 ± 1.8	13 ± 0	2.8 ± 0.2
Holothuroidea									
Psolus sp.	MT	SF	WB	4 (1)	8.3	-	21.9	17	2.2
Nemertea									
Amphiporus sp.	CB	CV	WB	6 (2)	10.2 ± 0.2	-22.8 ± 0.3	19.9 ± 0.4	34 ± 5	2.8 ± 0.1
Sipuncula									
Unidentified sipunculid sp. A	CB	DF	WB	4 (2)	5.2 ± 1.1	-	19.4 ± 0.4	11 ± 5	1.4 ± 0.3
	MT	DF	WB	7 (3)	6.2 ± 0.6	-	20 ± 0.3	13 ± 2	1.5 ± 0.2
Polychaeta									
Bylgides sp.	CB	CV	WB	7 (2)	12 ± 0.2	-20.6 ± 0.2	18.2	24 ± 1	3.4 ± 0
Bylgides sarsi	MT	CV	WB	7 (3)	11.2 ± 0.2	-22.2 ± 0.2	17.9 ± 0.2	54 ± 12	3 ± 0.1
Gattyana cirrhosa	CB	CV	WB	4 (2)	11.5 ± 0.1	-20.9 ± 0.3	20.5 ± 0.2	69 ± 25	3.2 ± 0
Harmothoe imbricata	CB	CV	WB	6 (2)	11 ± 0.6	-20.9 ± 0.8	17.8 ± 1.5	40 ± 3	3.1 ± 0.2
Nephtys sp.	MT	CV	WB	7 (3)	10.8 ± 0.4	-20.2 ± 0.4	17.3 ± 0.5	149 ± 58	2.9 ± 0.1
Nereis zonata	MT	DF	WB	3 (1)	8.7	-22.1	15.3	20	2.3
Pectinaria hyperborea	CB	DF	WB	4 (1)	7.1	-21.5	16.4	48	1.9
Phyllodoce groenlandica	CB	CV	WB	4 (2)	11.2 ± 0.2	-21 ± 0.4	17.4 ± 0.8	41 ± 11	3.1 ± 0
Unidentified polychaete sp.	MT	DF	WB	6 (3)	8.6 ± 0.7	-21.6 ± 0.1	15.3 ± 0.3	22 ± 2	2.2 ± 0.2

Taxon	Location	FG[a]	Tissue[b]	*n* ind (*n* comp)	$\delta^{15}N$ (‰)	$\delta^{13}C$ (‰)	$\delta^{34}S$ (‰)	MeHg (DW, ng/g)	TP
Bivalvia									
Astarte borealis	CB	SF	VM	8 (3)	9.2 ± 0.6	-22.4 ± 0.3	19.3 ± 0.4	32 ± 8	2.5 ± 0.2
Astarte sp.	CB	SF	VM	4 (2)	9.9 ± 0	-21.1 ± 0	20.8 ± 0.1	36 ± 2	2.7 ± 0
	MT	SF	VM	7 (3)	9.3 ± 0.1	-21.5 ± 1	20 ± 0.9	59 ± 12	2.5 ± 0
Clinocardium ciliatum	CB	SF	VM	3 (1)	9.2	-23.3	21.1	71	2.5
	MT	SF	VM	9 (3)	9.8 ± 1	-22.5 ± 0.2	19.7 ± 0.3	173 ± 55	2.6 ± 0.3
Cyclocardia sp.	MT	SF	VM	2 (1)	6.9	-21.8	19.9	89	1.8
Nuculana pernula	MT	DF	VM	4 (2)	9.2 ± 0.6	-23.3 ± 0.4	18.4 ± 0.2	47 ± 1	2.4 ± 0.2
Similipecten greenlandicus	CB	DF	VM	4 (1)	10.5	-21.5	21.1	76	2.9
	MT	DF	VM	16 (2)	10.8 ± 0.4	-23.8 ± 0.1	21.1 ± 0.3	146 ± 21	2.9 ± 0.1
Yoldia hyperborea	CB	DF	VM	3 (1)	8.1	-22.8	19.2	15	2.2
Gastropoda									
Boreotrophon truncatus	MT	CV	VM	3 (1)	9.7	-20.0	20.4	109	2.6
Buccinum polare	MT	CV	VM	5 (2)	11.2 ± 1.1	-20.5 ± 0.4	14.9 ± 4.8	172 ± 49	3 ± 0.3
Buccinum sp.	MT	CV	VM	5 (2)	9.9 ± 0.7	-21.7 ± 0.1	18.2 ± 0.7	89 ± 28	2.6 ± 0.2
Cryptonatica sp.	MT	CV	VM	6 (2)	10.5 ± 0.3	-20.8 ± 0.5	18.1 ± 0.5	141 ± 53	2.8 ± 0.1
Cylichna sp.	MT	CV	VM	3 (1)	8.4	-22.7	18.8	26	2.2
Margarites costalis	MT	DF	VM	8 (2)	10.7 ± 2.3	-21.6 ± 0.6	17.8 ± 1.6	61 ± 6	2.9 ± 0.7
Neptunea sp.	MT	CV	VM	5 (2)	10.5 ± 0.6	-20.3 ± 0.1	20.5 ± 0.3	268 ± 19	2.8 ± 0.2
Tachyrhynchus sp.	MT	CV	VM	2 (1)	5.9	-20.4	19.5	14	1.4
Nudibranchia									
Dendronotus frondosus	CB	CV	WB	5 (2)	13.7 ± 0.3	-22 ± 0.2	18.2 ± 0.6	42 ± 6	3.9 ± 0.1
	MT	CV	WB	3 (1)	8.6	-25.5	20.1	32	2.2

[a] Feeding guild: SF, suspension feeder; DF, deposit feeder; CV, carnivore. [b] Tissue: WB, whole body; VM, viscera and muscle; CD, central disk. [c] *A. behringiensis* were divided by size: L, large; S, small.

Trophic position and dietary indicators

Nitrogen stable isotope values were lowest in CB sipunculids (5.2 ± 1.1 ‰) and the MT gastropod *Tachyrhynchus* species (5.9 ‰). The highest $\delta^{15}N$ value (14.2 ‰) was found in the MT pycnogonids. Feeding guild and $\delta^{15}N$ were closely associated (two-way ANOVA, type III, accounting for location, FG $p < 0.0001$, $n = 147$) with deposit feeders and suspension feeders having significantly lower $\delta^{15}N$ values than carnivores (Tukey HSD, $p < 0.0001$ for both). Despite the difference in water column depth, the range of $\delta^{15}N$ values was similar at both sites. Methylmercury concentrations showed a strong linear relationship with $\delta^{15}N$ values at both locations (Figure 2.6A, two-site $\delta^{15}N$ slope = 0.14 ± 0.02, $r^2 = 0.37$, $p < 0.001$, $n = 147$).

The range of $\delta^{13}C$ values was greater at the MT site (-25.5 to -19.8‰) than at the CB site (-23.2 to -20.3‰). There was no difference between $\delta^{13}C$ values among feeding guilds though only a subset of samples were used in statistical tests owing to exclusion of animals containing carbonates. Carbon SI values were positively correlated with MeHg concentrations although it was not a strong explanatory variable in linear regressions (Figure 2.6B, two site $\delta^{13}C$ slope = 0.08, $r^2 = 0.07$, $p < 0.05$, $n = 71$).

Mean $\delta^{34}S$ values ranged from 14.9 ± 4.8 ‰ in the MT snail *Buccinum polare* to 26.8 ± 1.8 ‰ in the brittle star *Stegophiura nodosa*. Although much of the $\delta^{34}S$ range was shared between the two sites, the lowest individual $\delta^{34}S$ values were found in MT polychaetes (Unident. polychaete sp., 15 ‰) and MT snails (*B. polare*, 11.5 ‰). Methylmercury concentrations were not correlated to $\delta^{34}S$ values (Figure 2.6C) though

they differed between feeding guilds (two-way ANOVA, type III, accounting for location, feeding guild $p < 0.01$, $n = 145$).

Fatty acid composition varied considerably among the taxa analyzed. Of the 29 FA analytes, 10 FA were considered major (i.e., constituted greater than 5 % of TFA in more than one taxa) (Table 2.1). Generally, the major FAs responsible for the highest proportion of the total FA composition were C20:5n3 (26.7 ± 6.7 %), C16:1n7 (17.4 ± 10.1 %), C16:0 (15.7 ± 2.2 %) and C22:6n3 (11.1 ± 7.2 %). Between paired species, major fatty acid proportions were similar at the two locations, with the exceptions of the amphipod *A. beringiensis*, the polychaete *Bylgides sp.* and the unidentified sipunculids (Figure 2.7).

Copepod FABM were the only FABM to differ between feeding guilds (two-way ANOVA, type III with location, $p < 0.05$, $n = 62$) with significantly higher copepod FABM in carnivores than deposit feeders (Tukey HSD, $p < 0.005$). Bacteria and dinoflagellate FABM did not significantly vary by location or feeding guild. Aquatic FABM values were significantly higher at the CB location than at the MT site when controlling for feeding guild (two-way ANOVA, type III; location $p < 0.005$, $n = 62$) (Figure 2.8). Conversely, the terrestrial FABM was significantly higher for all feeding guilds at the MT site (two-way ANOVA, type III, location $p < 0.01$, $n = 62$). The CB invertebrates across all feeding guilds had higher diatom FABM than those at the MT site (two-way ANOVA, type III, location $p < 0.005$, $n = 62$) with significant differences found between deposit feeders and carnivores (Tukey HSD $p < 0.05$).

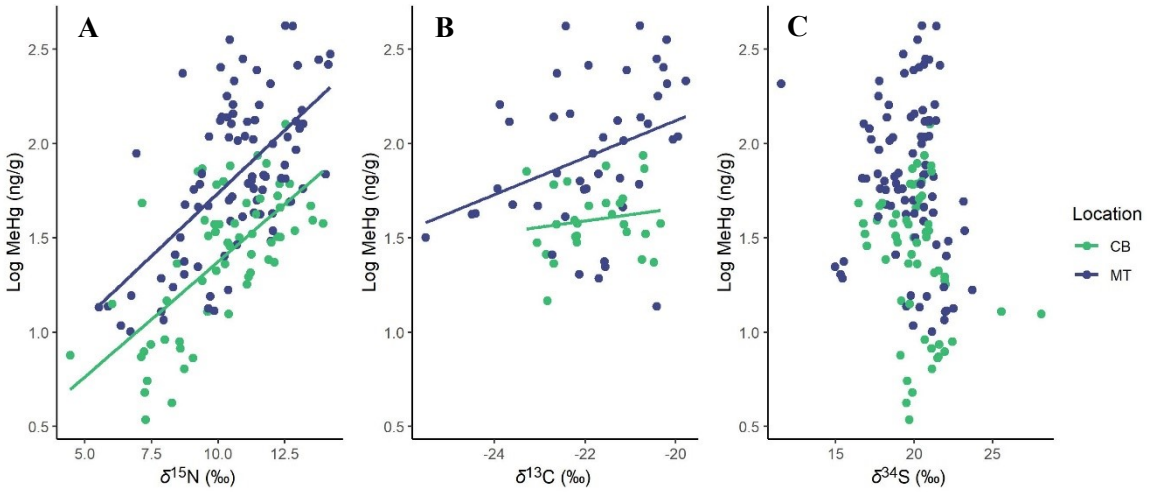

Figure 2.6. Scatter plots of MeHg concentrations in relation to A) $\delta^{15}N$, B) $\delta^{13}C$ and C) $\delta^{34}S$ with linear regression lines by location where applicable.

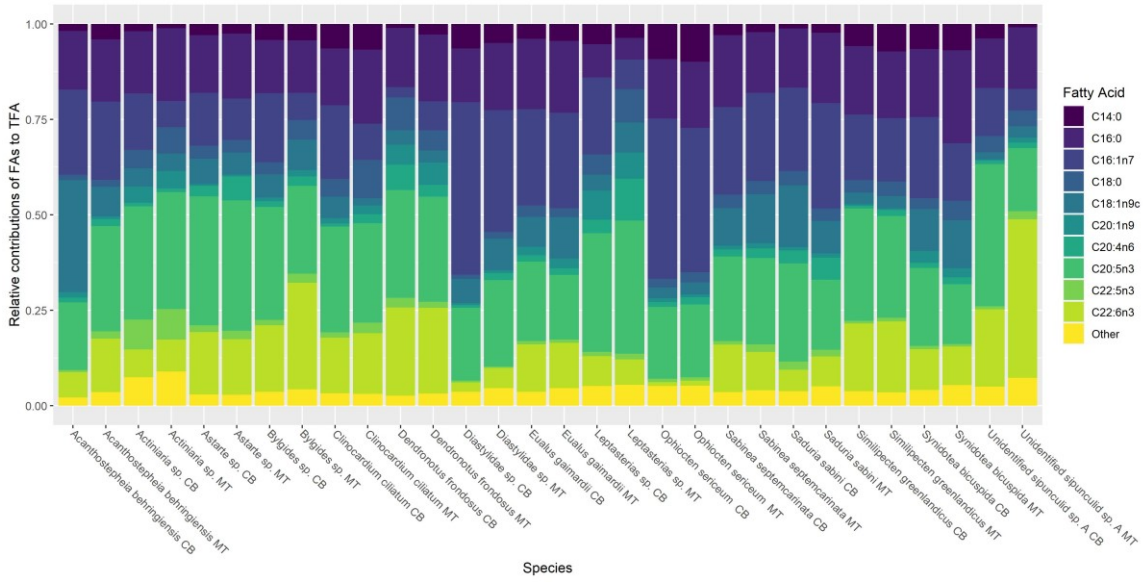

Figure 2.7. Stacked barplot for major FA contributions to TFA in paired species from Cape Bathurst (CB) and Mackenzie Trough (MT).

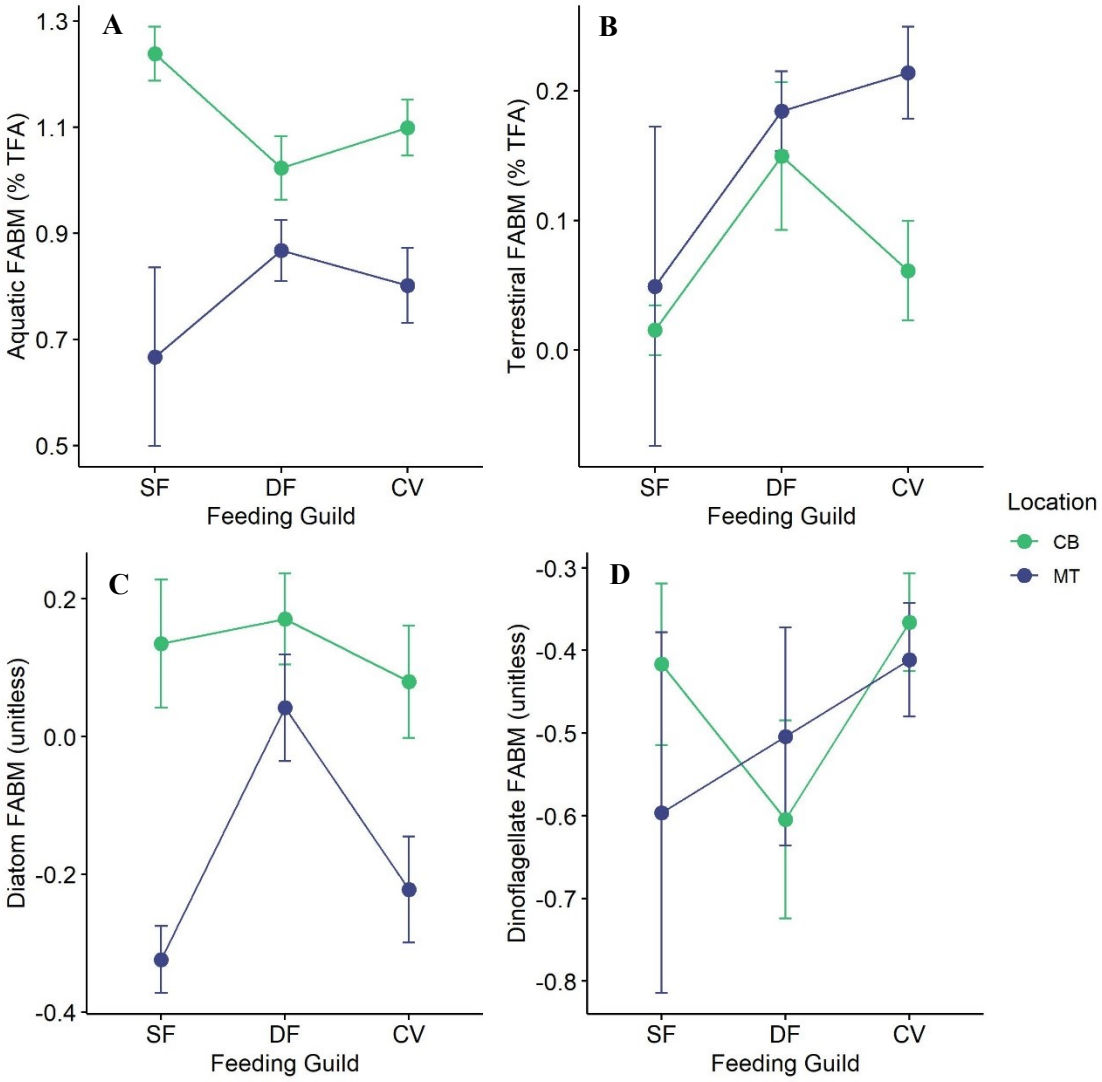

Figure 2.8. Two factor plots of mean log FABM (±SE) for A) aquatic, B) terrestrial, C) diatom and D) dinoflagellate indicators by feeding guild and location. (CV, carnivore; DF, deposit feeder; SF, suspension feeder).

Fatty acids and FABM were correlated to SIs and both explained MeHg concentrations in invertebrates. Strong positive Pearson correlations were found between $\delta^{15}N$ and C18:1n9c ($r = 0.53$, $p < 0.001$), C20:1n9 ($r = 0.44$, $p < 0.05$) and copepod FABM ($r = 0.423$, $p < 0.05$), all of which are indicative of a carnivorous diet (Table 2.5). The correlation between $\delta^{34}S$ values and C22:5n3 was strongly negative indicating that dinoflagellate FA decreased with more aquatic foraging locations ($r = -0.53$, $p < 0.005$). Methylmercury concentration was negatively correlated to diatom related FA (C16:1n7, $r = -0.49$, $p < 0.005$) and FABM ($r = -0.44$, $p <0.05$). Methylmercury correlations were both positively and negatively correlated to dietary indicators. The two negative correlations both involved variables that related to diatom feeding (C16:1n7, $r = -0.49$, $p <0.005$; diatom FABM, $r = -0.44$, $p < 0.05$). Meanwhile MeHg concentration were positively associated with a benthic diet, indicated by C20:4n6 ($r = 0.42$, $p < 0.05$) and a dinoflagellate-based feeding indicated by C22:5n3 ($r = 0.44$, $p < 0.05$).

Univariate linear modelling for invertebrate MeHg concentrations revealed linear correlations with seven FAs, see Figure 2.9. Diatom-related FAs C14:0 and C16:1n7 were negatively related to MeHg concentrations ($r^2 = 0.1$, $p < 0.05$, and $r^2 = 0.24$, $p < 0.001$, respectively, $n = 62$ for both). Positive linear relationships between MeHg concentrations were found in all dinoflagellate-related FAs (C18:0, $r^2 = 0.12$, $p < 0.01$; C22:5n3, $r^2 = 0.2$, $p < 0.001$; C22:6n3, $r^2 = 0.09$, $p < 0.05$; $n = 62$ for all FAs). The indicator of benthic food sources, C20:4n6, also had positive correlation with MeHg concentration ($r^2 = 0.18$, $p < 0.001$, $n = 62$). Diatom and dinoflagellate FABM had weak linear relationships with MeHg concentrations (diatom FABM, $r^2 = 0.19$, $p < 0.005$;

dinoflagellate FABM, $r^2 = 0.07$, $p < 0.05$; $n = 62$ for both, Figure 2.10). No significant relationship was found between MeHg concentrations and the concentrations of terrestrial, bacteria or copepod FABM.

Table 2.5. Pearson correlations between FA/FABM proportions and either SI values or MeHg concentration (*n* = number of samples), coefficients (*r*) and Holm-Bonferroni (α = 0.05) corrected *p*-values.

FA/FABM	Variable	*n*	*r*	*p*-value
Log C18:1n9c (%TFA)	$\delta^{15}N$	62	0.53	0.0006
Log C22:5n3 (%TFA)	$\delta^{34}S$	61	-0.53	0.0010
Log C16:1n7 (%TFA)	Log MeHg	62	-0.49	0.0034
Log C20:1n9 (%TFA)	$\delta^{15}N$	62	0.44	0.0179
Log C22:5n3 (%TFA)	Log MeHg	62	0.44	0.0196
Log Diatom FABM	Log MeHg	62	-0.44	0.0231
Log C20:4n6 (%TFA)	Log MeHg	62	0.42	0.0388
Log Copepod FABM (%TFA)	$\delta^{15}N$	62	0.42	0.0434

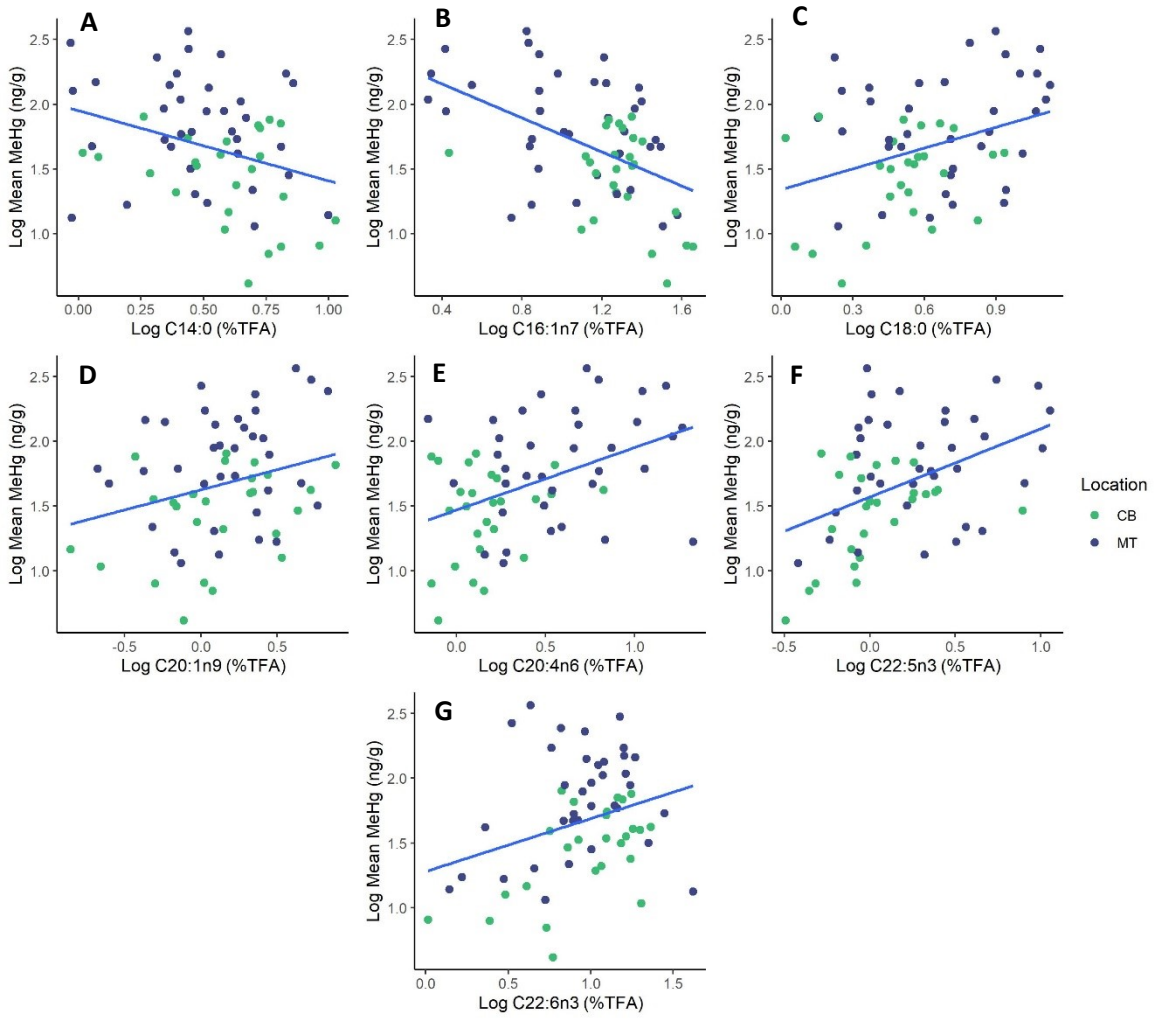

Figure 2.9. Scatter plots with regression lines for log MeHg concentrations with respect to log transformed proportions of FAs: A) C14:0, B) C16:1n7, C) C18:0, D) C20:1n9, E) C20:4n6, F) C22:5n3 and G) C22:6n3.

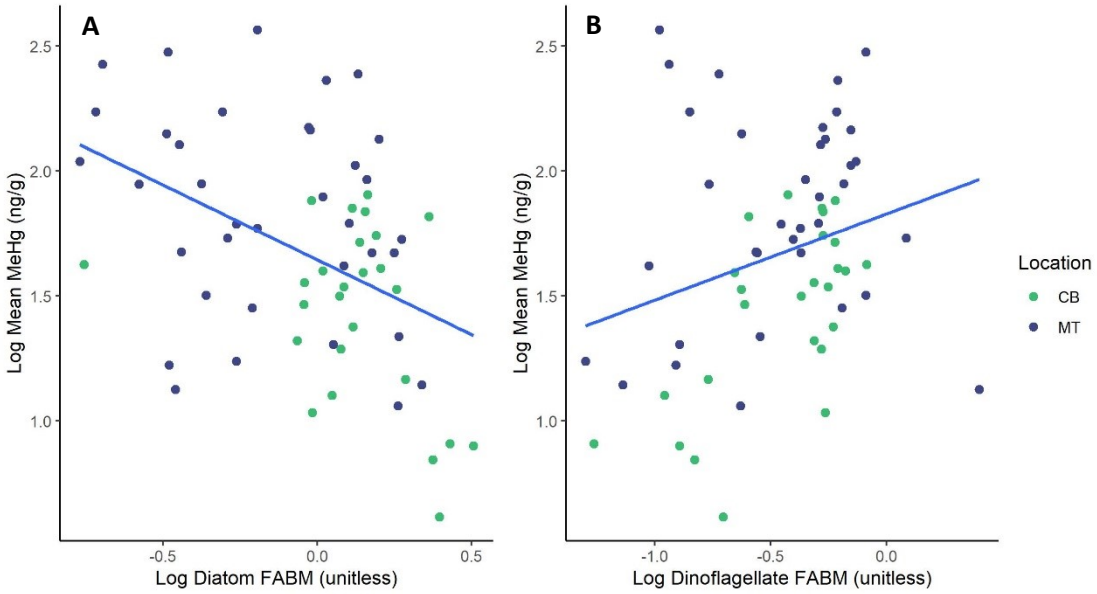

Figure 2.10. Scatterplots with regression lines for log mean MeHg concentrations with respect to A) log diatom and B) log dinoflagellate FABMs.

Models for MeHg accumulation

The multivariate model that best explained variation in benthic invertebrate MeHg concentration included logC16:0, logC18:1n9c, logC22:6n3, mean $\delta^{15}N$ values and location variables ($r^2 = 0.69$, $p < 0.005$, $n = 62$) (Table 2.6). Location and $\delta^{15}N$ values were the strongest explanatory variables according to multiple linear regressions of all possible combinations of explanatory variables. The same three FAs were significant explanatory variables in both models that included FAs: C16:0 ($p < 0.005$) and C18:1n9c ($p < 0.05$), both indicative of carnivory; and C22:6n3, indicative of dinoflagellate diet ($p < 0.05$). Diatom FABM was the only FABM that explained a significant amount of variation in MeHg concentrations (data set 3, partial $r^2 = 0.12$, $p <$ 0.05) but it should be noted that it was only significant in the absence of stable isotope explanatory variables. Data set variables, best models, Akaike's Information Criterion (adjusted for small sample size, AICc) and parameters are found in Table 2.6. Note that due to differences in sample size, the AICc values simply reflect the best AICc for model fit of each data set and are not comparable to each other.

Table 2.6. Parameters of multiple regression models for MeHg concentration, number of samples in model (*n*) for four subsets of the data that included different explanatory variables. Note that location and feeding guild were included as explanatory variables in each data subset.

Model	Variables in best model	Partial r^2	Model r^2	AICc	*p*-value
All MeHg data (n = 145)	$\delta^{15}N$	0.34	0.55	74.7	$< 2.2 \times 10^{-16}$
	Location	0.17			
	$\delta^{34}S$	0.03			
All samples with $\delta^{13}C$ data (n = 70)[a]	Location	0.24	0.58	8.2	1.10×10^{-11}
	$\delta^{15}N$	0.12			
	$\delta^{13}C$	0.11			
	$\delta^{34}S$	0.11			
All FA and FABM (n = 62)	Location	0.17	0.46	50.3	1.33×10^{-6}
	Diatom FABM	0.13			
	Log C22:6n3	0.07			
	Log C16:0	0.06			
	Log C18:1n9c	0.03			
Mean $\delta^{15}N$, mean $\delta^{34}S$, all FA and FABM (n = 62)	Mean $\delta^{15}N$	0.32	0.69	16.2	4.81×10^{-13}
	Location	0.21			
	Log C22:6n3	0.08			
	Log C16:0	0.06			
	Log C18:1n9c	0.02			

[a] $\delta^{13}C$ for this model includes values only from invertebrate tissues with low/no carbonate composition.

Principal component analyses

PCAs using log ratio transformed major FAs and log transformed FABM illustrated slight differences in dietary sources between the two study locations (Figure 2.11). Neither the FA nor the FABM PCA showed differences in dietary sources related to feeding guild. In the FA PCA, the first two PCs accounted for 53.7 % of the FA variation within the benthic invertebrates studied. PC1 was positively associated with C18:0 and C22:5n3, both of which are linked to dinoflagellate-based diets, and negatively associated with C16:1n7, a FA indicative of diatom-based food sources. PC2 was characterized by C20:5n3, a diatom FA, along the positive axis and the copepod FA, C20:1n9, along the negative axis. The location-based confidence ellipses suggest that benthic invertebrates at the CB site relied more heavily on diatoms whereas benthic invertebrates at the MT site incorporated more dinoflagellates in their diets. In the FABM PCA, PC1 and PC2 account for 54.5 % of the FABM variation in the dataset. The first PC is positively correlated with FAs originating from terrestrial organic matter and bacteria while negatively correlated with aquatic and diatom FAs. The positive PC2 axis is correlated with dinoflagellate diets whereas the negative PC2 axis is associated with diatom-based diets. Similar to the FA PCA, the location-based confidence ellipses reflect a more aquatic and diatom based food web at the CB site. Benthic invertebrates at the MT site however, used more terrestrial and bacteria based food sources.

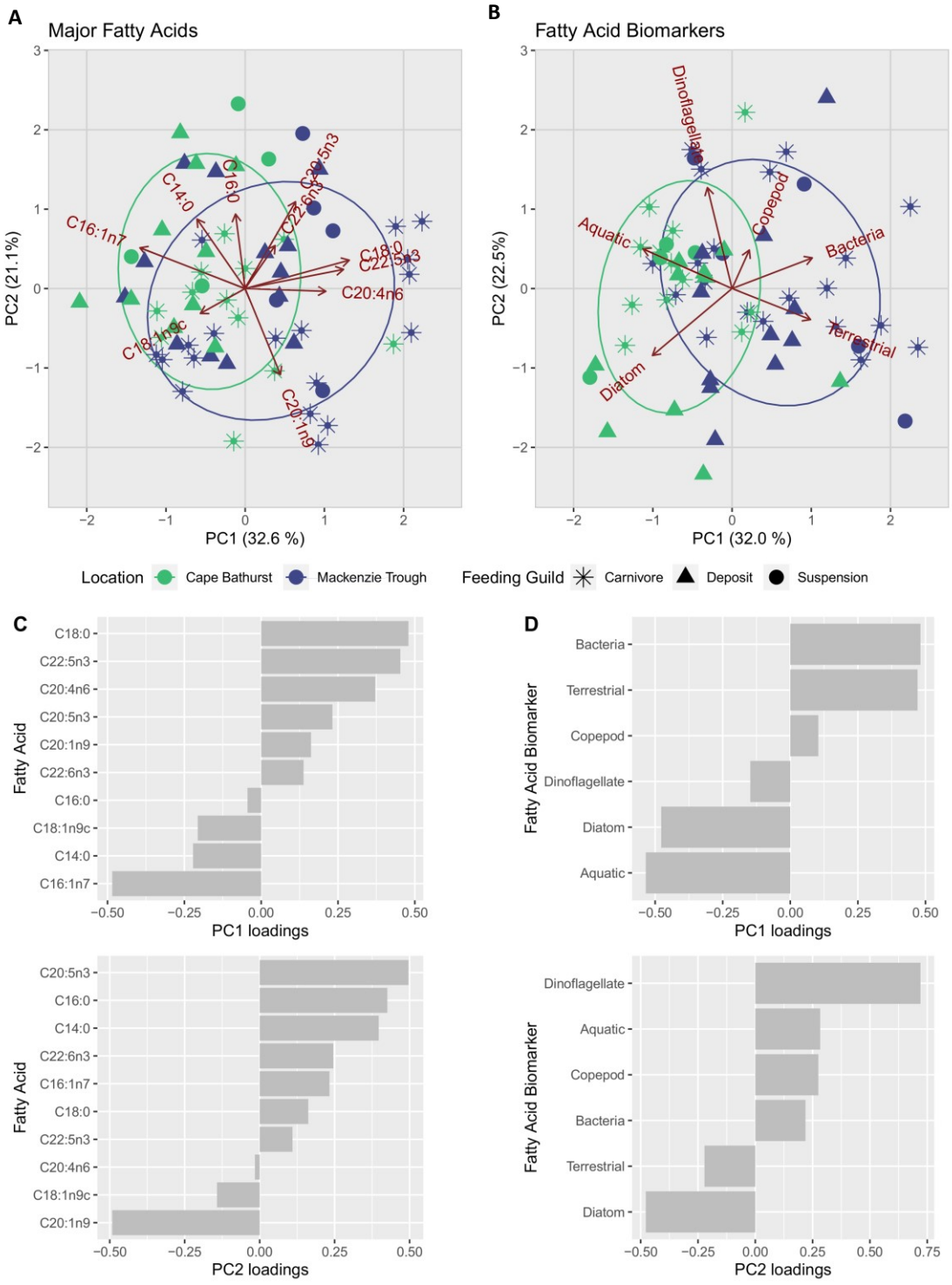

Figure 2.11. Bi-plots of PCAs for A) major fatty acids and B) fatty acid biomarkers and associated PC1 and PC2 loadings for variability in C) major fatty acids and D) fatty acid biomarkers.

Discussion

This study demonstrates that invertebrate MeHg concentrations vary widely among taxa and are strongly influenced by trophic position, location and diet. Trophic position was the dominant explanatory variable, reflecting the importance of biomagnification. Variation in organic matter sources to the benthic food webs had a small but significant effect on MeHg accumulation as well. This study also suggests benthic marine invertebrates are exposed to more MeHg at the Mackenzie Trough location than at the Cape Bathurst location.

Methylmercury in CBS benthic food webs

MeHg concentrations in the benthic invertebrates of this study varied by two orders of magnitude over three trophic levels. The highest MeHg concentrations in this study, found in the carnivorous sunstar *C. papposus*, are comparable to or greater than dry weight MeHg concentrations in animals typically considered higher in the food web such as ringed seal, seabirds and pelagic fish (Campbell et al., 2005; Riget et al., 2007; Loseto et al., 2008; Burham et al., 2018). Although limited information is available for toxicological effects of MeHg on marine invertebrates, the concentrations observed in this study are below known critical body burdens associated with a risk of effects seen in Arctic fish and invertebrates (Barst et al., 2022).

The influence of trophic position and feeding guild on MeHg concentration

Carnivores had significantly higher $\delta^{15}N$ values and MeHg concentrations which was expected given their higher trophic position. While carnivores did have higher MeHg concentrations in this study, other studies have found that aquatic invertebrates feeding on detritus or sedimentary deposits had higher Hg accumulation rates than predatory

invertebrates suggesting that bioavailability of MeHg can vary within habitat zones within a specific location (Boudou and Ribeyre, 1995; Sizmur et al., 2013).

Statistical investigations into the effect of feeding guild on MeHg uptake highlighted correlations between feeding guild and certain individual dietary indicators. As seen in Mohan et al. (2016), there were differences in FA and FABM with respect to differential feeding modes. Copepod FABM and FAs that indicate copepod predation (C18:1n9c and C20:1n9) were not correlated to MeHg concentrations however they were significantly higher in carnivores than deposit or suspension feeders. Few studies have investigated the relationship between FAs and mercury accumulation so comparison of correlations is limited. However, both McMeans et al. (2015) and Liu et al. (2020) found C18:1n9c alone or as part of an FABM explained a portion of MeHg accumulation in marine food webs.

Fatty acids and FABMs indicative of diatom-based diets were negatively correlated with MeHg concentrations and were highest in deposit feeders. Contrarily, the FABM for another main phytoplankton group of the Arctic Ocean, dinoflagellates, was positively correlated to MeHg concentration. It is possible this difference is due to the fact that, unlike diatoms, dinoflagellates can be heterotrophic and can use colloidal matter as food sources (Lee et al., 2016). As such dinoflagellates could have increased exposure to metals bound to terrestrial organic matter used for energy (Tranvik et al., 1993).

The $\delta^{15}N$ values of the animals in this study were comparable to those in other Arctic Ocean studies (Hobson et al. 2002; Connelly et al., 2014; Stasko et al., 2018). The linear relationship between $\delta^{15}N$ and log MeHg demonstrated a mean trophic magnification slope (TMS) of 0.14 (SE ± 0.02) which is comparable to the average polar marine MeHg TMS of 0.21 (SD ± 0.09) from Lavoie et al. (2013). These results differ from those of Atwell (1998) who found that trophic position was an insignificant determinant of Hg concentration in Arctic marine invertebrates within comparable $\delta^{15}N$ ranges to those in this study. The difference in depth between the two locations (CB, 22 m; MT, 116 m) did not influence the $\delta^{15}N$ values of the animals in this study; an outcome contrary to Stasko et al. (2018) who found that $\delta^{15}N$ values increased with depth across the shelf of the CBS. It should be noted, however, that their study examined the influence of water depth over a much broader depth range (20-500 m). The $\delta^{15}N$ of invertebrates was a significant independent variable in all of the multiple linear regression models that included stable isotopes as a predictor of MeHg concentrations. When $\delta^{15}N$ was controlled for, location was shown to significantly influence of MeHg accumulation.

The influence of location on MeHg accumulation

Carbon SI, FA and FABM highlighted spatial variation in the types of organic matter sources available at the two locations. On the other hand, sulfur isotope values in the CBS benthic food web did not vary significantly between locations and could not be used to explain differences in MeHg uptake. Conceivably, the strictly benthic nature of the animals analyzed prevented the variation required to observe relationships between $\delta^{34}S$ and mercury accumulation seen in other studies (Elliot and Elliot, 2016; Willacker et al., 2017; Góngora et al., 2018). While a relationship with MeHg concentration was not

observed in this study, $\delta^{34}S$ values did demonstrate that deposit feeders had significantly higher signatures than carnivores and that $\delta^{34}S$ values were positively correlated with dinoflagellate-based diets. Seawater has a $\delta^{34}S$ value of approximately 21 ‰ (Tostevin et al., 2014) and many of the taxa in this study had $\delta^{34}S$ signature comparable to that of seawater. There were some taxa however that strayed from the seawater benchmark; for instance, the $\delta^{34}S$ value of the CB deposit-feeding brittle star (*S. nodosa,* 26.8 ± 1.8 ‰) was higher than seawater as well as higher than the $\delta^{34}S$ value of *S. nodosa* in other invertebrate $\delta^{34}S$ studies (Góngora et al., 2018; Reinhart et al., 2018). The lowest $\delta^{34}S$ value in this study was found in the MT carnivorous snail (*B. polare*, 14.9 ± 4.8 ‰), indicating either the availability of freshwater and/or terrestrial energy sources linked to Mackenzie River input, or the influence of sulfate reduction in sediments.

The low $\delta^{34}S$ values found in the MT taxa, potentially indicating the influence of freshwater inputs from the Mackenzie River, is corroborated by the lower $\delta^{13}C$ values found in the same taxa. The differing carbon SI ranges at the two sites suggests that the benthic invertebrates at the MT site had access to a wider variety of carbon sources than those at the CB site. The results of this study agree with those of Morata et al. (2008) and Connelly et al. (2012) in which sedimentary $\delta^{13}C$ values varied across the CBS and were slightly lower near the Mackenzie River delta. The FABM marker for terrestrial organic matter sources was also higher in MT invertebrates, further confirming that the MT food web relies to some extent on energy sources carried by the Mackenzie River. Bacterial FABM were also higher in taxa at the MT site. These FABM mirror results of Connelly et al. (2012) for sites closer to the Mackenzie River delta. Organic material in the

Mackenzie River was observed to contain bacteria, microalgae and vascular plants (Yunker et al., 1995). Recent studies have also shown that much of the particulate matter in the Mackenzie River is comprised of old carbon, likely released from eroding permafrost (Campeau et al., 2022). Fatty acid biomarkers indicate that the CB invertebrates relied more heavily on aquatic energy sources, with significant reliance on diatom-based food pathways. The $\delta^{13}C$ signatures of CB benthic taxa also reflect marine carbon sources, due to the higher values. It is possible that since CB is shallow and within the euphotic zone, both benthic and sympagic diatoms may be significant energy resources.

Dietary indicators, other than $\delta^{15}N$, explained a small amount of MeHg accumulation in the invertebrates. The environmental processes behind local differences in MeHg uptake could be attributed to physical differences between the two sites that affect the amount of MeHg available to benthic invertebrates. Location was statistically significant in every predicative model of MeHg concentrations, accounting for 30-41 % of the ability of the model to account for the variability in MeHg concentrations. Of the 30 samples with highest MeHg concentration in this study, 29 were collected in the Mackenzie Trough site. Admittedly, contrasting two locations does not allow for investigation into the drivers of spatial MeHg accumulation patterns. It does however support other spatial study findings of variable MeHg concentrations in the Arctic Ocean (Brown et al,. 2016; St. Louis et al., 2017; Wang et al., 2018).

The grain size of sediment can influence its mercury content. Fox et al. (2014) found that sediments with a higher proportion of silt and clay than sand were associated with higher sediment concentrations of THg in the Chukchi Sea. Grain size measurements were provided by K. Conlan (CMN) for sites near the sampling locations of this study (also taken in the summer of 2007 from the CCGS Nahidik). The proportion of silt and clay at the CB site (74.2 %) was higher than that of the MT site (60.2 %) therefore, based on grain size alone, there is higher potential for mercury in the sediment at the CB site. Although positive correlations have been previously reported between sediment THg and benthic invertebrate MeHg concentrations (Désy et al. 2000; Chen et al., 2014), sediment THg was not measured in this study.

The Arctic Ocean demonstrates significant stratification of water masses of with variable concentrations of MeHg (Wang et al., 2018). The difference in depth between the two locations could also affect the amount of MeHg available to the benthic taxa. Soerensen et al. (2016) reported that the polar mixed layer which is found between 20 m and 200 m depth in the Beaufort Sea, had lower MeHg concentrations than the surface layer. However, in the Wang et al. (2018) study, deeper waters, at approximately 400 m depth in the CBS, had the highest MeHg concentrations in the whole of the Canadian Arctic Ocean. Some studies suggest that elevated MeHg concentrations in the Canadian Arctic Ocean is due higher influxes of riverine inorganic Hg (Leitch et al., 2007; Wang et al., 2018). Wang et al. (2018), however, also suggest that the high seawater MeHg concentrations of the CBS may be due to water masses from the Bering Strait and Chukchi Sea that entered the CBS within the upper haloclines.

The chemical processes controlling methylation rates in benthic habitats were not included as variables in this study. Including such measurements as sediment dissolved oxygen, temperature and THg might have increased the ability of the multivariate models to explain spatial variability in the invertebrate MeHg concentrations. The dissimilarity of depth between the two locations may have influenced the oxygenation of the sediment which could in turn affect methylation rates and ultimately the amount of MeHg available to the invertebrates collected from each site. Bottom water temperature readings were not taken at the sites in this study, however numerous research expeditions between 2002 and 2006 recorded 67 bottom water temperature measurements at other sites on Mackenzie Shelf of the Beaufort Sea within a depth range of 20-120 m (unpublished data; K. Conlan). The range in temperature was -1.6°C to 0.5°C, suggesting that variation in temperature was minimal and may not play an influential role in the variability of MeHg production between the two study sites. Future studies integrating THg concentrations in sediment with invertebrate MeHg concentrations may further clarify patterns in THg/MeHg distributions within the Beaufort Sea.

The influx of THg is strongly associated to river discharge and proximity to major rivers has been shown to increase the amount of THg in marine sediments (Fitzgerald et al., 2007; Leitch et al., 2007). The proximity to the Mackenzie River delta therefore could plausibly contribute to the higher MeHg concentrations in the MT invertebrates of this study. The Mackenzie River delivers 249–333 km^3 of freshwater to the CBS annually (Dittmar and Kattner, 2003). The freshwater plume extends up to 70 km north of the coastline, carrying approximately 130 megatons of sediment annually (Carson et al.,

1998; Majewski et al., 2017), see Figure 2.1. Over the span of 2007-2010, the Mackenzie River annual output contained an estimated 1850−3400 kg of Hg, including 15−23 kg of MeHg (Emmerton et al., 2013). Leitch et al. (2007) found that approximately 50% of the seaward Hg entered the CBS during the spring freshet, a period of immense productivity, and concluded that the Mackenzie River is the largest source of Hg to the Beaufort Sea.

In this study, the biomagnification of MeHg with trophic position was expected. Somewhat surprising was the rivalling importance of location to MeHg accumulation. With dietary variation between locations only accounting for a minor amount of MeHg accumulation and TMS similar between the two locations, our results suggest that there are spatial differences in the amount of MeHg available to benthic invertebrates of the CBS. This is particularly relevant considering that some of the highest Hg concentrations in Arctic marine mammals have been reported for the Beaufort Sea region (Brown et al., 2016; St. Louis et al., 2017; Brown et al., 2018). Identifying the underlying causes of the spatial influences in this study was limited due to the fact that only two locations were assessed however the Mackenzie River might be a significant source of THg leading to locally high concentrations of MeHg. Further studies to elucidate MeHg accumulation spatial patterns within the shallow CBS would be useful, especially when taking into account proximity to the Mackenzie River as a variable. In addition, temporal patterns investigating the possible relationship between Mackenzie River annual output and annual fluctuations in local taxa MeHg concentrations may help determine the extent of the influence of riverine Hg sources on MeHg accumulation in marine biota.

Conclusion

This study provides the most comprehensive data on MeHg concentrations in Arctic marine benthic invertebrates to date. The use of traditional and genetic taxonomy strengthened the validity of the food web interactions illustrated by both stable isotope and fatty acid analyses. Trophic position of CBS benthic taxa was strongly associated with higher MeHg concentrations. Methylmercury biomagnification was corroborated by carnivory-associated FAs. Trends in bioaccumulation of MeHg vary food source, suggesting that phytoplanktonic diversity may play a minor role in MeHg uptake to food webs. Species-specific examination of dietary indicators illustrated that energy sources in the CBS were spatially variable and suggest that proximity to freshwater resources of the Mackenzie River influences dietary pathways. While providing a baseline for future MeHg concentrations monitoring, this study also highlights the need for further investigation into the influence of the Mackenzie River on Beaufort Sea benthic invertebrate ecology.

Chapter 3

General discussion and future directions

Collectively, our understanding of how mercury impacts wildlife is well-developed but knowledge gaps exist in our understanding of mercury dynamics at the base of food webs (Pomerleau et al., 2016; Loria et al., 2020). This study adds valuable information to the understanding of MeHg dynamics at the base of the food web in the CBS by highlighting the influence of feeding guild, diet and location on MeHg accumulation in benthic invertebrates. Describing the processes that influence MeHg uptake in marine food webs is a necessary first step for predicting how MeHg dynamics and food webs may change under future scenarios (Poste et al., 2019; Zhang et al., 2021).

Climate change is predicted to influence the ways MeHg enters Arctic marine food webs (Box et al., 2019; Stadnyk et al., 2020). Methylmercury inputs are expected to be variably affected by changes in sea ice regimes, increased freshwater influx, increased suspended organic matter, ocean acidification, and changes to oceanographic currents. All of these factors will alter the sources and amounts of organic matter reaching the seafloor and the seasonal timing of such settlements (Søreide et al., 2013; Dutkiewicz et al., 2015; Yunda-Guarin et al., 2021).

This work also has highlighted our limited understanding of MeHg dynamics with respect to spatial and temporal scales. Future work could, for example, obtain MeHg concentrations of invertebrates collected from a larger number of sites with increasing latitudinal and longitudinal distance from the Mackenzie River delta. Such information can be used to evaluate the likelihood that Mackenzie River influx is a major driver of spatial variation in Hg and/or MeHg biotic concentrations on the Mackenzie Shelf of the CBS. Radiocarbon dating of invertebrates could be used to illustrate the age of the dietary carbon supporting the invertebrates and might identify locations where older terrestrial

carbon sources are being assimilated into marine invertebrate diets (Ishikawa et al. 2020; Campeau et al., 2021). This could be particularly important as recent Hg isotope evidence indicates that MeHg bioaccumulation in marine animals may be linked to Hg of terrestrial origin (AMAP, 2021). In addition, the Mackenzie River plume extent and annual discharge data could be used to assess whether fluctuations in the amount of riverine Hg entering the CBS is reflected in inter-annual variation of MeHg concentrations in both pelagic and benthic invertebrates. As climate change increases the amount of mercury being transported to the Arctic Ocean, it is becoming even more important to determine the fate of this mercury load on bioaccumulation in the marine food web.

References

AMAP, 2011. Mercury in the Arctic, Climate Change 2013 - The Physical Science Basis. Oslo, Norway.

AMAP, 2021. AMAP Assessment 2021: Mercury in the Arctic. Arctic Monitoring and Assessment Programme (AMAP), Tromsø, Norway. 324 pp

Atwell, L., Hobson, K.A., Welch, H.E., 1998. Biomagnification and bioaccumulation of mercury in an arctic marine food web: insights from stable nitrogen isotope analysis. Can. J. Fish. Aquat. Sci 55, 1114–1121.

Barst, BD, J Chételat, N Basu. 2022. Toxicological risk of mercury for fish and invertebrate prey in the Arctic. Science of the Total Environment, in review.

Bilyard, G.R., 1987. The value of benthic infauna in marine pollution monitoring studies, Marine Pollution Bulletin. Number I I.

Bligh, E.G., Dyer, W.J., 1959. A rapid method of total lipid extraction and purification. Can. J. Biochem. Physiol. 37, 911–917. https://doi.org/10.1139/o59-099

Bodin, N., Le Loc'h, F., Hily, C., 2007. Effect of lipid removal on carbon and nitrogen stable isotope ratios in crustacean tissues. J. Exp. Mar. Bio. Ecol. 341, 168–175. https://doi.org/10.1016/j.jembe.2006.09.008

Boudou, A., Ribeyre, F., 1997. Mercury in the food web: accumulation and transfer mechanisms, in: Sigel, A., Sigel, H. (Eds.), Metal Ions in Biological Systems. Marcel Dekker, Inc., New York, pp. 289–319.

Bourgeois, S., Archambault, P., Witte, U., 2017. Organic matter remineralization in marine sediments: A Pan-Arctic synthesis. Global Biogeochem. Cycles 31, 190–213. https://doi.org/10.1002/2016GB005378

Box, J.E., Colgan, W.T., Christensen, T.R., Schmidt, N.M., Lund, M., Parmentier,

F.J.W., Brown, R., Bhatt, U.S., Euskirchen, E.S., Romanovsky, V.E., Walsh, J.E., Overland, J.E., Wang, M., Corell, R.W., Meier, W.N., Wouters, B., Mernild, S., Mård, J., Pawlak, J., Olsen, M.S., 2019. Key indicators of Arctic climate change: 1971-2017. Environ. Res. Lett. https://doi.org/10.1088/1748-9326/aafc1b

Braune, B., Chételat, J., Amyot, M., Brown, T., Clayden, M., Evans, M., Fisk, A., Gaden, A., Girard, C., Hare, A., Kirk, J., Lehnherr, I., Letcher, R., Loseto, L., Macdonald, R., Mann, E., McMeans, B., Muir, D., O'Driscoll, N., Poulain, A., Reimer, K., Stern, G., 2015. Mercury in the marine environment of the Canadian Arctic: Review of recent findings. Sci. Total Environ. 509–510, 67–90. https://doi.org/10.1016/j.scitotenv.2014.05.133

Brown, T.M., Fisk, A.T., Wang, X., Ferguson, S.H., Young, B.G., Reimer, K.J., Muir, D.C.G., 2016. Mercury and cadmium in ringed seals in the Canadian Arctic: Influence of location and diet. Sci. Total Environ. 545–546, 503–511. https://doi.org/10.1016/j.scitotenv.2015.12.030

Brown, T.M., Macdonald, R.W., Muir, D.C.G., Letcher, R.J., 2018. The distribution and trends of persistent organic pollutants and mercury in marine mammals from Canada's Eastern Arctic. Sci. Total Environ. 618, 500-517. https://doi.org/10.1016/j.scitotenv.2017.11.052

Budge, S.M., Iverson, S.J., Koopman, H.N., 2006. Studying trophic ecology in marine ecosystems using fatty acids: A primer on analysis and interpretation. Mar. Mammal Sci. 22, 759–801. https://doi.org/10.1111/j.1748-7692.2006.00079.x

Burnham, J.H., Burnham, K.K., Chumchal, M.M., Welker, J.M., Johnson, J.A., 2018. Correspondence between mercury and stable isotopes in high Arctic marine and

terrestrial avian species from northwest Greenland. Polar Biol. 41, 1475–1491. https://doi.org/10.1007/s00300-018-2302-9

Campbell, L.M., Norstrom, R.J., Hobson, K.A., Muir, D.C.G., Backus, S., Fisk, A.T., 2005. Mercury and other trace elements in a pelagic Arctic marine food web (Northwater Polynya, Baffin Bay). Sci. Total Environ. 351–352, 247–263. https://doi.org/10.1016/j.scitotenv.2005.02.043

Campeau, A., Eklöf, K., Soerensen, A.L., Åkerblom, S., Yuan, S., Hintelmann, H., Bieroza, M., Köhler, S., Zdanowicz, C., 2022. Sources of riverine mercury across the Mackenzie River Basin; inferences from a combined Hg C isotopes and optical properties approach. Sci. Total Environ. 806, 150808. https://doi.org/10.1016/j.scitotenv.2021.150808

Carmack, E.C., Kulikov, E.A., 1998. Wind-forced upwelling and internal Kelvin wave generation in Mackenzie Canyon, Beaufort Sea. J. Geophys. Res. Ocean. 103. https://doi.org/10.1029/98JC00113

Carmack, E.C., Macdonald, R.W., 2002. Oceanography of the Canadian shelf of the Beaufort Sea: A setting for marine life. Arctic 55, 29–45. https://doi.org/10.14430/arctic733

Carson, M.A., Jasper, J.N., Conly, F.M., 1998. Magnitude and sources of sediment input to the Mackenzie Delta, Northwest Territories, 1974-94. Arctic 51, 116–124.

Celo, V., Lean, D.R.S., Scott, S.L., 2006. Abiotic methylation of mercury in the aquatic environment. Sci. Total Environ. 368, 126–137. https://doi.org/10.1016/j.scitotenv.2005.09.043

Chen, C., Amirbahman, A., Fisher, N., Harding, G., Lamborg, C., Nacci, D., Taylor, D.,

2008. Methylmercury in marine ecosystems: Spatial patterns and processes of production, bioaccumulation, and biomagnification. Ecohealth 5, 399–408. https://doi.org/10.1007/s10393-008-0201-1

Chen, C.Y., Borsuk, M.E., Bugge, D.M., Hollweg, T., Balcom, P.H., Ward, D.M., Williams, J., Mason, R.P., 2014. Benthic and pelagic pathways of methylmercury bioaccumulation in estuarine food webs of the Northeast United States. PLoS One 9. https://doi.org/10.1371/journal.pone.0089305

Chételat, J., Ackerman, J.T., Eagles-Smith, C.A., Hebert, C.E., 2020. Methylmercury exposure in wildlife: A review of the ecological and physiological processes affecting contaminant concentrations and their interpretation. Sci. Total Environ. 711, 135117. https://doi.org/10.1016/j.scitotenv.2019.135117

Chételat, J., McKinney, M.A., Amyot, M., Dastoor, A., Douglas, T.A., Heimbürger-Boavida, L.E., Kirk, J., Kahilainen, K.K., Outridge, P.M., Pelletier, N., Skov, H., St. Pierre, K., Vuorenmaa, J., Wang, F., 2022. Climate change and mercury in the Arctic: Abiotic interactions. Sci. Total Environ. 824. https://doi.org/10.1016/j.scitotenv.2022.153715

Clayden, M.G., Arsenault, L.M., Kidd, K.A., O'Driscoll, N.J., Mallory, M.L., 2015. Mercury bioaccumulation and biomagnification in a small Arctic polynya ecosystem. Sci. Total Environ. 509–510, 206–215. https://doi.org/10.1016/j.scitotenv.2014.07.087

Coelho, J.P., Mieiro, C.L., Pereira, E., Duarte, A.C., Pardal, M.A., 2013. Mercury biomagnification in a contaminated estuary food web: Effects of age and trophic position using stable isotope analyses. Mar. Pollut. Bull. 69, 110–115.

https://doi.org/10.1016/j.marpolbul.2013.01.021

Compeau, G.C., Bartha, R., 1985. Sulfate-reducing bacteria: principal methylators of mercury in anoxic estuarine sediment. Appl. Environ. Microbiol. 50, 498–502.

Conlan, K., Aitken, A., Hendrycks, E., McClelland, C., Melling, H., 2008. Distribution patterns of Canadian Beaufort Shelf macrobenthos. J. Mar. Syst. 74, 864–886. https://doi.org/10.1016/j.jmarsys.2007.10.002

Conlan, K., Hendrycks, E., Aitken, A., Williams, B., Blasco, S., Crawford, E., 2013. Macrofaunal biomass distribution on the Canadian Beaufort Shelf. J. Mar. Syst. 127, 76–87. https://doi.org/10.1016/j.jmarsys.2013.07.013

Connelly, T.L., Deibel, D., Parrish, C.C., 2014. Trophic interactions in the benthic boundary layer of the Beaufort Sea shelf, Arctic Ocean: Combining bulk stable isotope and fatty acid signatures. Prog. Oceanogr. 120, 79–92. https://doi.org/10.1016/j.pocean.2013.07.032

Connelly, T.L., Deibel, D., Parrish, C.C., 2012a. Elemental composition, total lipid content, and lipid class proportions in zooplankton from the benthic boundary layer of the Beaufort Sea shelf (Canadian Arctic). Polar Biol. 35, 941–957. https://doi.org/10.1007/s00300-011-1142-7

Connelly, T.L., Deibel, D., Parrish, C.C., 2012b. Biogeochemistry of near-bottom suspended particulate matter of the Beaufort Sea shelf (Arctic Ocean): C, N, P, δ 13C and fatty acids. Cont. Shelf Res. 43, 120–132. https://doi.org/10.1016/j.csr.2012.05.011

Connolly, R.M., Guest, M.A., Melville, A.J., Oakes, J.M., 2004. Sulfur stable isotopes separate producers in marine food-web analysis. Oecologia 138, 161–167.

https://doi.org/10.1007/s00442-003-1415-0

Córdoba-Tovar, L., Marrugo-Negrete, J., Barón, P.R., Díez, S., 2022. Drivers of biomagnification of Hg, As and Se in aquatic food webs: A review. Environ. Res. 204. https://doi.org/10.1016/j.envres.2021.112226

Cossa, D., Gobeil, C., 2000. Mercury speciation in the Lower St. Lawrence Estuary. Can. J. Fish. Aquat. Sci. 57.

Dalsgaard, J., St. John, M., Kattner, G., Müller-Navarra, D., Hagen, W., 2003. Fatty acid trophic markers in the pelagic marine environment. Adv. Mar. Biol. 46, 225–340. https://doi.org/10.1016/S0065-2881(03)46005-7

de la Vega, C., Jeffreys, R.M., Tuerena, R., Ganeshram, R., Mahaffey, C., 2019. Temporal and spatial trends in marine carbon isotopes in the Arctic Ocean and implications for food web studies. Glob. Chang. Biol. 25, 4116–4130. https://doi.org/10.1111/gcb.14832

Désy, J.C., Archambault, J.-F., Pinel-Alloul, B., Hubert, J., Campbell, P.G.C., 2000. Relationships between total mercury in sediments and methyl mercury in the freshwater gastropod prosobranch Bithynia tentaculata in the St. Lawrence River, Quebec. Can. J. Fish. Aquat. Sci.

Dietz, R., Outridge, P.M., Hobson, K.A., 2009. Anthropogenic contributions to mercury levels in present-day Arctic animals-A review. Sci. Total Environ. 407, 6120–6131. https://doi.org/10.1016/j.scitotenv.2009.08.036

Dittmar, T., Kattner, G., 2003. The biogeochemistry of the river and shelf ecosystem of the Arctic Ocean: A review. Mar. Chem. 83, 103–120. https://doi.org/10.1016/S0304-4203(03)00105-1

Douglas, T.A., Loseto, L.L., MacDonald, R.W., Outridge, P., Dommergue, A., Poulain, A., Amyot, M., Barkay, T., Berg, T., Chetelat, J., Constant, P., Evans, M., Ferrari, C., Gantner, N., Johnson, M.S., Kirk, J., Kroer, N., Larose, C., Lean, D., Nielsen, T.G., Poissant, L., Rognerud, S., Skov, H., Sørensen, S., Wang, F., Wilson, S., Zdanowicz, C.M., 2012. The fate of mercury in Arctic terrestrial and aquatic ecosystems, a review. Environ. Chem. 9, 321–355. https://doi.org/10.1071/EN11140

Dutkiewicz, S., Morris, J.J., Follows, M.J., Scott, J., Levitan, O., Dyhrman, S.T., Berman-Frank, I., 2015. Impact of ocean acidification on the structure of future phytoplankton communities. Nat. Clim. Chang. 5, 1002–1006. https://doi.org/10.1038/nclimate2722

Eagles-Smith, C.A., Suchanek, T.H., Colwell, A.E., Anderson, N.L., 2008. Mercury trophic transfer in a eutrophic lake: The importance of habitat-specific foraging. Ecol. Appl. 18. https://doi.org/10.1890/06-1476.1

Edwards, G., 1865. Two cases of poisoning by mercuric methide (methylmercury). Saint Bartholomew's Hosp Rep 1, 141–150.

Elliott, K.H., Elliott, J.E., 2016. Origin of sulfur in diet drives spatial and temporal mercury trends in seabird eggs from pacific Canada 1968−2015. Environ. Sci. Technol. 50, 13380–13386. https://doi.org/10.1021/acs.est.6b05458

Emmerton, C.A., Graydon, J.A., Gareis, J.A.L., St. Louis, V.L., Lesack, L.F.W., Banack, J.K.A., Hicks, F., Nafziger, J., 2013. Mercury export to the Arctic Ocean from the Mackenzie River, Canada. Environ. Sci. Technol. 47, 7644–7654. https://doi.org/10.1021/es400715r

Evers, D., 2018. Encyclopedia of the Anthropocene, in: Dellasala, D.A., Goldstein, M.I.

(Eds.), Encyclopedia of the Anthropocene. pp. 181–194.

Falk-Petersen, S., Sargent, J.R., Tande, K.S., 1987. Lipid composition of zooplankton in relation to the sub-Arctic food web. Polar Biol 8, 115–120.

Fitzgerald, W.F., Lamborg, C.H., Hammerschmidt, C.R., 2007. Marine biogeochemical cycling of mercury. Chem. Rev. 107, 641–662. https://doi.org/10.1021/cr050353m

Fox, A.L., Hughes, E.A., Trocine, R.P., Trefry, J.H., Schonberg, S. V., McTigue, N.D., Lasorsa, B.K., Konar, B., Cooper, L.W., 2014. Mercury in the northeastern Chukchi Sea: Distribution patterns in seawater and sediments and biomagnification in the benthic food web. Deep. Res. Part II Top. Stud. Oceanogr. 102, 56–67. https://doi.org/10.1016/j.dsr2.2013.07.012

Fry, B., 2006. Stable Isotope Ecology. Springer, New York.

Fry, B., Chumchal, M.M., 2011. Sulfur stable isotope indicators of residency in estuarine fish. Limnol. Oceanogr. 56, 1563–1576. https://doi.org/10.4319/lo.2011.56.5.1563

Góngora, E., Braune, B.M., Elliott, K.H., 2018. Nitrogen and sulfur isotopes predict variation in mercury levels in Arctic seabird prey. Mar. Pollut. Bull. 135, 907–914. https://doi.org/10.1016/j.marpolbul.2018.07.075

Graeve, M., Kattner, G., Piepenburg, D., 1997. Lipids in arctic benthos: Does the fatty acid and alcohol composition reflect feeding and trophic interactions? Polar Biol. 18, 53–61. https://doi.org/10.1007/s003000050158

Griffiths, J.R., Kadin, M., Nascimento, F.J.A., Tamelander, T., Törnroos, A., Bonaglia, S., Bonsdorff, E., Brüchert, V., Gårdmark, A., Järnström, M., Kotta, J., Lindegren, M., Nordström, M.C., Norkko, A., Olsson, J., Weigel, B., Žydelis, R., Blenckner, T., Niiranen, S., Winder, M., 2017. The importance of benthic–pelagic coupling for

marine ecosystem functioning in a changing world. Glob. Chang. Biol. 23, 2179–2196. https://doi.org/10.1111/gcb.13642

Habicht, K.S., Canfield, D.E., Rethmeier, J.J., 1998. Sulfur isotope fractionation during bacterial reduction and disproportionation of thiosulfate and sulfite. Geochim. Cosmochim. Acta 62, 2585–2595.

Harding, G., Dalziel, J., Vass, P., 2018. Bioaccumulation of methylmercury within the marine food web of the outer Bay of Fundy, Gulf of Maine. PLoS One 13. https://doi.org/10.1371/journal.pone.0197220

Hebert, C.E., Arts, M.T., Weseloh, D.V.C., 2006. Ecological tracers can quantify food web structure and change. Environ. Sci. Technol. 40, 5618–5623. https://doi.org/10.1021/es0520619

Hebert, C.E., Popp, B.N., 2018. Temporal trends in a biomagnifying contaminant: Application of amino acid compound-specific stable nitrogen isotope analysis to the interpretation of bird mercury levels. Environ. Toxicol. Chem. 37, 1458–1465. https://doi.org/10.1002/etc.4092

Hecky, R.E., Hesslein, R.H., 1995. Contributions of benthic algae to lake food webs as revealed by stable isotope analysis. Am. Benthol. Soc 14, 631–653.

Hobson, K.A., 1999. Tracing origins and migration of wildlife using stable isotopes: a review. Oecologia 120, 314–326. https://doi.org/10.1007/s004420050865

Hoover, C., Giraldo, C., Ehrman, A., Suchy, K.D., MacPhee, S.A., Brewster, J., Reist, J.D., Power, M., Swanson, H., Loseto, L., 2022. The Canadian Beaufort Shelf trophic structure: evaluating an ecosystem modelling approach by comparison with observed stable isotopic structure. Arct. Sci. 8, 292–312. https://doi.org/10.1139/as-

2020-0035

Ishikawa, N.F., Finlay, J.C., Uno, H., Ogawa, N.O., Ohkouchi, N., Tayasu, I., Power, M.E., 2020. Combined use of radiocarbon and stable carbon isotopes for the source mixing model in a stream food web. Limnol. Oceanogr. 65, 2688–2696. https://doi.org/10.1002/lno.11541

Ivanova, N. V., Dewaard, J.R., Hebert, P.D.N., 2006. An inexpensive, automation-friendly protocol for recovering high-quality DNA. Mol. Ecol. Notes 6, 998–1002. https://doi.org/10.1111/j.1471-8286.2006.01428.x

Iverson, S.J., Field, C., Don Bowen, W., Blanchard, W., 2004. Quantitative fatty acids signature analysis: A new method of estimating predator diets. Ecol. Monogr. 74, 211–235.

Jacob, U., Mintenbeck, K., Brey, T., Knust, R., Beyer, K., 2005. Stable isotope food web studies: A case for standardized sample treatment. Mar. Ecol. Prog. Ser. 287, 251–253. https://doi.org/10.3354/meps287251

Jennings, S., Warr, K.J., 2003. Environmental correlates of large-scale spatial variation in the δ15N of marine animals. Mar. Biol. 142, 1131–1140. https://doi.org/10.1007/s00227-003-1020-0

Kehrig, H.A., Seixas, T.G., Baêta, A.P., Malm, O., Moreira, I., 2010. Inorganic and methylmercury: Do they transfer along a tropical coastal food web? Mar. Pollut. Bull. 60, 2350–2356. https://doi.org/10.1016/j.marpolbul.2010.08.010

Kelly, J.R., Scheibling, R.E., 2012. Fatty acids as dietary tracers in benthic food webs. Mar. Ecol. Prog. Ser. 446, 1–22. https://doi.org/10.3354/meps09559

Kirk, J.L., Lehnherr, I., Andersson, M., Braune, B.M., Chan, L., Dastoor, A.P., Durnford,

D., Gleason, A.L., Loseto, L.L., Steffen, A., St. Louis, V.L., 2012. Mercury in Arctic marine ecosystems: Sources, pathways and exposure. Environ. Res. 119, 64–87. https://doi.org/10.1016/j.envres.2012.08.012

Lansard, B., Mucci, A., Miller, L.A., MacDonald, R.W., Gratton, Y., 2012. Seasonal variability of water mass distribution in the southeastern Beaufort Sea determined by total alkalinity and δ18O. J. Geophys. Res. Ocean. 117. https://doi.org/10.1029/2011JC007299

Lavoie, R.A., Hebert, C.E., Rail, J.F., Braune, B.M., Yumvihoze, E., Hill, L.G., Lean, D.R.S., 2010. Trophic structure and mercury distribution in a Gulf of St. Lawrence (Canada) food web using stable isotope analysis. Sci. Total Environ. 408, 5529–5539. https://doi.org/10.1016/j.scitotenv.2010.07.053

Lavoie, R.A., Jardine, T.D., Chumchal, M.M., Kidd, K.A., Campbell, L.M., 2013. Biomagnification of mercury in aquatic food webs: A worldwide meta-analysis. Environ. Sci. Technol. 47, 13385–13394. https://doi.org/10.1021/es403103t

Lee, C.S., Fisher, N.S., 2016. Methylmercury uptake by diverse marine phytoplankton. Limnol. Oceanogr. 61, 1626–1639. https://doi.org/10.1002/lno.10318

Legeżyńska, J., Kędra, M., Walkusz, W., 2014. Identifying trophic relationships within the high Arctic benthic community: How much can fatty acids tell? Mar. Biol. 161, 821–836. https://doi.org/10.1007/s00227-013-2380-8

Lehnherr, I., 2014. Methylmercury biogeochemistry: a review with special reference to Arctic aquatic ecosystems. Environ. Rev. 22, 229–243. https://doi.org/10.1139/er-2013-0059

Lehnherr, I., St. Louis, V.L., Hintelmann, H., Kirk, J.L., 2011. Methylation of inorganic

mercury in polar marine waters. Nat. Geosci. 4, 298–302. https://doi.org/10.1038/ngeo1134

Leitch, D.R., Carrie, J., Lean, D., Macdonald, R.W., Stern, G.A., Wang, F., 2007. The delivery of mercury to the Beaufort Sea of the Arctic Ocean by the Mackenzie River. Sci. Total Environ. 373, 178–195. https://doi.org/10.1016/j.scitotenv.2006.10.041

Leveillé, J.-C., Amblard, C., Bourdier, G., 1997. Fatty acids as specific algal markers in a natural lacustrian phytoplankton. J. Plankton Res. 19, 469–490.

Liu, M., Xiao, W., Zhang, Q., Shi, L., Wang, X., Xu, Y., 2020. Methylmercury bioaccumulation in deepest ocean fauna: Implications for ocean mercury biotransport through food webs. Environ. Sci. Technol. Lett. 7, 469–476. https://doi.org/10.1021/acs.estlett.0c00299

Lobo, J., Costa, P.M., Teixeira, M.A.L., Ferreira, M.S.G., Costa, M.H., Costa, F.O., 2013. Enhanced primers for amplification of DNA barcodes from a broad range of marine metazoans. BMC Ecol. 13. https://doi.org/10.1186/1472-6785-13-34

Loria, A., Archambault, P., Burt, A., Ehrman, A., Grant, C., Power, M., Stern, G.A., 2020. Mercury and stable isotope (δ13C and δ15N) trends in decapods of the Beaufort Sea. Polar Biol. 43, 443–456. https://doi.org/10.1007/s00300-020-02646-x

Loseto, L.L., Stern, G.A., Deibel, D., Connelly, T.L., Prokopowicz, A., Lean, D.R.S., Fortier, L., Ferguson, S.H., 2008a. Linking mercury exposure to habitat and feeding behaviour in Beaufort Sea beluga whales. J. Mar. Syst. 74, 1012–1024. https://doi.org/10.1016/j.jmarsys.2007.10.004

Loseto, L.L., Stern, G.A., Ferguson, S.H., 2008b. Size and biomagnification: How habitat

selection explains beluga mercury levels. Environ. Sci. Technol. 42, 3982–3988. https://doi.org/10.1021/es7024388

Lovvorn, J.R., North, C.A., Grebmeier, J.M., Cooper, L.W., Kolts, J.M., 2018. Sediment organic carbon integrates changing environmental conditions to predict benthic assemblages in shallow Arctic seas. Aquat. Conserv. Mar. Freshw. Ecosyst. 28, 861–871. https://doi.org/10.1002/aqc.2906

Macdonald, R.W., Loseto, L.L., 2010. Are Arctic Ocean ecosystems exceptionally vulnerable to global emissions of mercury? A call for emphasised research on methylation and the consequences of climate change. Environ. Chem. 7, 133–138. https://doi.org/10.1071/EN09127

Macdonald, T.A., Burd, B.J., Macdonald, V.I., Van Roodselaar, A., 2010. Taxonomic and feeding guild classification for the marine benthic macroinvertebrates of the Strait of Georgia, British Columbia. Can. Tech. Rep. Fish. Aquat. Sci. 2874.

Majewski, A.R., Atchison, S., MacPhee, S., Eert, J., Niemi, A., Michel, C., Reist, J.D., 2017. Marine fish community structure and habitat associations on the Canadian Beaufort shelf and slope. Deep. Res. Part I Oceanogr. Res. Pap. 121, 169–182. https://doi.org/10.1016/j.dsr.2017.01.009

Majewski, A.R., Lowdon, M.K., Reist, J.D., Park, B.J., 2011. Fish catch data from Herschel Island, Yukon Territory, and other offshore sites in the Canadian Beaufort Sea, July and August 2007, aboard the CCGS Nahidik. Can. Data Rep. Fish. Aquat. Sci. 1231.

Majewski, A.R., Reist, J.D., Park, B.J., Sareault, J.E., Lowdon, M.K., 2009. Fish catch data from offshore sites in the Mackenzie River estuary and Beaufort Sea during the

open water season, July and August, 2005, aboard the CCGS Nahidik. Can. Data Rep. Fish. Aquat. Sci.

Marziali, L., Roscioli, C., Valsecchi, L., 2021. Mercury bioaccumulation in benthic invertebrates: From riverine sediments to higher trophic levels. Toxics 9. https://doi.org/10.3390/toxics9090197

Mason, R.P., Reinfelder, J.R., Morel, F.M.M., 1996. Uptake, toxicity, and trophic transfer of mercury in a coastal diatom. Environ. Sci. Technol. 30, 1835–1845. https://doi.org/10.1021/es950373d

McMeans, B.C., Arts, M.T., Fisk, A.T., 2015. Impacts of food web structure and feeding behavior on mercury exposure in Greenland Sharks (Somniosus microcephalus). Sci. Total Environ. 509–510, 216–225. https://doi.org/10.1016/j.scitotenv.2014.01.128

Middelburg, J.J., Herman, P.M.J., 2007. Organic matter processing in tidal estuaries. Mar. Chem. 106, 127–147. https://doi.org/10.1016/j.marchem.2006.02.007

Minagawa, M., Wada, E., 1984. Stepwise enrichment of 15N along food chains: Further evidence and the relation between δ15N and animal age. Geochim. Cosmochim. Acta 48, 1135–1140. https://doi.org/10.1016/0016-7037(84)90204-7

Mohan, S.D., Connelly, T.L., Harris, C.M., Dunton, K.H., Mcclelland, J.W., 2016. Seasonal trophic linkages in Arctic marine invertebrates assessed via fatty acids and compound-specific stable isotopes. Ecosphere 7. https://doi.org/10.1002/ecs2.1429

Morata, N., Renaud, P.E., Brugel, S., Hobson, K.A., Johnson, B.J., 2008. Spatial and seasonal variations in the pelagic-benthic coupling of the southeastern Beaufort Sea revealed by sedimentary biomarkers. Mar. Ecol. Prog. Ser. 371, 47–63. https://doi.org/10.3354/meps07677

Morel, F.M.M., Kraepiel, A.M.L., Amyot, M., 1998. The chemical cycle and bioaccumulation of mercury, Annu. Rev. Ecol. Syst.

National Research Council, 2000. Toxicological effects of methylmercury. National Academies Press, Washington, D.C. https://doi.org/10.17226/9899

Outridge, P.M., MacDonald, R.W., Wang, F., Stern, G.A., Dastoor, A.P., 2008. A mass balance inventory of mercury in the Arctic Ocean. Environ. Chem. 5, 89–111. https://doi.org/10.1071/EN08002

Parrish, C.C., Abrajano, T.A., Budge, S.M., Helleur, R.J., Hudson, E.D., Pulchan, K., Ramos, C., 2000. Lipid and phenolic biomarkers in marine ecosystems: Analysis and applications, in: Wangersky, P. (Ed.), The Handbook of Environmental Chemistry: Marine Chemistry. Springer-Verlag, Berlin Heidelberg, pp. 193–223. https://doi.org/10.1007/10683826_8

Parzanini, C., Parrish, C.C., Hamel, J.F., Mercier, A., 2019. Reviews and syntheses: Insights into deep-sea food webs and global environmental gradients revealed by stable isotope (δ15N, δ13C) and fatty acid trophic biomarkers. Biogeosciences 16, 2837–2856. https://doi.org/10.5194/bg-16-2837-2019

Peterson, B.J., Fry, B., 1987. Stable isotopes in ecosystem studies. Attn. Rev. Ecol. Syst 18, 293–320.

Piepenburg, D., Ambrose, W.G., Brandt, A., Renaud, P.E., Ahrens, M.J., Jensen, P., 1997. Benthic community patterns reflect water column processes in the Northeast Water polynya (Greenland). J. Mar. Syst. 10, 467–482. https://doi.org/10.1016/S0924-7963(96)00050-4

Pomerleau, C., Stern, G.A., Pućko, M., Foster, K.L., Macdonald, R.W., Fortier, L., 2016.

Pan-Arctic concentrations of mercury and stable isotope ratios of carbon (δ13C) and nitrogen (δ15N) in marine zooplankton. Sci. Total Environ. 551–552, 92–100. https://doi.org/10.1016/j.scitotenv.2016.01.172

Post, D.M., 2002. Using stable isotopes to estimate trophic position: Models, methods, and assumptions. Ecology 83, 703–718. https://doi.org/10.2307/3071875

Poste, A.E., Hoel, C.S., Andersen, T., Arts, M.T., Færøvig, P.J., Borgå, K., 2019. Terrestrial organic matter increases zooplankton methylmercury accumulation in a brown-water boreal lake. Sci. Total Environ. 674, 9–18. https://doi.org/10.1016/j.scitotenv.2019.03.446

Rigét, F., Møller, P., Dietz, R., Nielsen, T.G., Asmund, G., Strand, J., Larsen, M.M., Hobson, K.A., 2007. Transfer of mercury in the marine food web of West Greenland. J. Environ. Monit. 9, 877–883. https://doi.org/10.1039/b704796g

Routti, H., Letcher, R.J., Born, E.W., Branigan, M., Dietz, R., Evans, T.J., Fisk, A.T., Peacock, E., Sonne, C., 2011. Spatial and temporal trends of selected trace elements in liver tissue from polar bears (Ursus maritimus) from Alaska, Canada and Greenland. J. Environ. Monit. 13, 2260–2267. https://doi.org/10.1039/c1em10088b

Schell, D., Barnett, B., Vinette, K., 1998. Carbon and nitrogen isotope ratios in zooplankton of the Bering, Chukchi and Beaufort seas. Mar. Ecol. Prog. Ser. 162, 11–23. https://doi.org/10.3354/meps162011

Scheuhammer, A.M., Basu, N., Evers, D.C., Heinz, G.H., Sandheinrich, M.B., Bank, M.S., 2012. Ecotoxicology of mercury in fish and wildlife: Recent advances, in: Mercury in the Environment. University of California Press, pp. 223–238. https://doi.org/10.1525/california/9780520271630.003.0011

Schlechtriem, C., Henderson, R.J., Tocher, D.R., 2008. A critical assessment of different transmethylation procedures commonly employed in the fatty acid analysis of aquatic organisms. Limnol. Oceanogr. Methods 6, 523–531. https://doi.org/10.4319/lom.2008.6.523

Sizmur, T., Canário, J., Edmonds, S., Godfrey, A., O'Driscoll, N.J., 2013. The polychaete worm Nereis diversicolor increases mercury lability and methylation in intertidal mudflats. Environ. Toxicol. Chem. 32, 1888–1895. https://doi.org/10.1002/etc.2264

Soerensen, A.L., Jacob, D.J., Schartup, A.T., Fisher, J.A., Lehnherr, I., St Louis, V.L., Heimbürger, L.E., Sonke, J.E., Krabbenhoft, D.P., Sunderland, E.M., 2016. A mass budget for mercury and methylmercury in the Arctic Ocean. Global Biogeochem. Cycles 30, 560–575. https://doi.org/10.1002/2015GB005280

Søreide, J.E., Carroll, M.L., Hop, H., Ambrose, W.G., Hegseth, E.N., Falk-Petersen, S., 2013. Sympagic-pelagic-benthic coupling in Arctic and Atlantic waters around Svalbard revealed by stable isotopic and fatty acid tracers. Mar. Biol. Res. 9, 831–850. https://doi.org/10.1080/17451000.2013.775457

St. Louis, V.L., Derocher, A.E., Stirling, I., Graydon, J.A., Lee, C., Jocksch, E., Richardson, E., Ghorpade, S., Kwan, A.K., Kirk, J.L., Lehnherr, I., Swanson, H.K., 2011. Differences in mercury bioaccumulation between polar bears (Ursus maritimus) from the Canadian high- and sub-arctic. Environ. Sci. Technol. 45, 5922–5928. https://doi.org/10.1021/es2000672

Stadnyk, T.A., Tefs, A., Broesky, M., Déry, S.J., Myers, P.G., Ridenour, N.A., Koenig, K., Vonderbank, L., Gustafsson, D., 2021. Changing freshwater contributions to the Arctic: A 90-year trend analysis (1981- 2070). Elementa 9.

https://doi.org/10.1525/elementa.2020.00098

Stasko, A.D., Bluhm, B.A., Reist, J.D., Swanson, H., Power, M., 2018. Relationships between depth and δ15N of Arctic benthos vary among regions and trophic functional groups. Deep. Res. Part I Oceanogr. Res. Pap. 135, 56–64. https://doi.org/10.1016/j.dsr.2018.03.010

Steffen, A., Douglas, T., Amyot, M., Ariya, P., Aspmo, K., Berg, T., Bottenheim, J., Brooks, S., Cobbett, F., Dastoor, A., Dommergue, A., Ebinghaus, R., Ferrari, C., Gardfeldt, K., Goodsite, M.E., Lean, D., Poulain, A.J., Scherz, C., Skov, H., Sommar, J., Temme, C., 2008. A synthesis of atmospheric mercury depletion event chemistry in the atmosphere and snow. Atmos. Chem. Phys 8, 1445–1482.

Steffen, A., Lehnherr, I., Cole, A., Ariya, P., Dastoor, A., Durnford, D., Kirk, J., Pilote, M., 2015. Atmospheric mercury in the Canadian Arctic. Part I: A review of recent field measurements. Sci. Total Environ. 509–510, 3–15. https://doi.org/10.1016/j.scitotenv.2014.10.109

Stern, G.A., Macdonald, R.W., 2005. Biogeographic provinces of total and methyl mercury in zooplankton and fish from the Beaufort and Chukchi Seas: Results from the SHEBA drift. Environ. Sci. Technol. 39, 4707–4713. https://doi.org/10.1021/es0482278

Stern, G.A., Macdonald, R.W., Outridge, P.M., Wilson, S., Chételat, J., Cole, A., Hintelmann, H., Loseto, L.L., Steffen, A., Wang, F., Zdanowicz, C., 2012. How does climate change influence Arctic mercury? Sci. Total Environ. 414, 22–42. https://doi.org/10.1016/j.scitotenv.2011.10.039

Stowasser, G., McAllen, R., Pierce, G.J., Collins, M.A., Moffat, C.F., Priede, I.G., Pond,

D.W., 2009. Trophic position of deep-sea fish-assessment through fatty acid and stable isotope analyses. Deep. Res. Part I Oceanogr. Res. Pap. 56, 812–826. https://doi.org/10.1016/j.dsr.2008.12.016

Tostevin, R., Turchyn, A. V., Farquhar, J., Johnston, D.T., Eldridge, D.L., Bishop, J.K.B., McIlvin, M., 2014. Multiple sulfur isotope constraints on the modern sulfur cycle. Earth Planet. Sci. Lett. 396, 14–21. https://doi.org/10.1016/j.epsl.2014.03.057

Tranvik, L., Sherr, E., Sherr, B., 1993. Uptake and utilization of "colloidal DOM" by heterotrophic flagellates in seawater. Mar. Ecol. Prog. Ser. 92, 301–309. https://doi.org/10.3354/meps092301

Ullrich, S.M., Tanton, T.W., Abdrashitova, S.A., 2001. Mercury in the aquatic environment: A review of factors affecting methylation. Crit. Rev. Environ. Sci. Technol. 31, 241–293.

United Nations Environment Programme, 2018. Global Mercury Assessment.

Vander Zanden, J., Rasmussen, J., 2001. Variation of d15N and d13C trophic fractionation: Implications for aquatic food web studies. Limnol. Oceanogr. 46, 2061–2066.

Wang, F., MacDonald, R.W., Armstrong, D.A., Stern, G.A., 2012. Total and methylated mercury in the Beaufort Sea: The role of local and recent organic remineralization. Environ. Sci. Technol. 46, 11821–11828. https://doi.org/10.1021/es302882d

Wang, K., Munson, K.M., Beaupré-Laperrière, A., Mucci, A., Macdonald, R.W., Wang, F., 2018. Subsurface seawater methylmercury maximum explains biotic mercury concentrations in the Canadian Arctic. Sci. Rep. 8. https://doi.org/10.1038/s41598-018-32760-0

Whitehouse, G.A., Buckley, T.W., Danielson, S.L., 2017. Diet compositions and trophic guild structure of the eastern Chukchi Sea demersal fish community. Deep Sea Res. Part II Top. Stud. Oceanogr. 135, 95–110. https://doi.org/10.1016/j.dsr2.2016.03.010

Willacker, J.J., Eagles-Smith, C.A., Ackerman, J.T., 2017. Mercury bioaccumulation in estuarine fishes: Novel insights from sulfur stable isotopes. Environ. Sci. Technol. 51, 2131–2139. https://doi.org/10.1021/acs.est.6b05325

Williams, W.J., Carmack, E.C., 2008. Combined effect of wind-forcing and isobath divergence on upwelling at Cape Bathurst, Beaufort Sea. J. Mar. Res. 66, 645–663.

World Health Organization, 2017. Mercury and Health [WWW Document]. https://www.who.int/news-room/fact-sheets/detail/mercury-and-health.

Yunda-Guarin, G., Brown, T.A., Michel, L.N., Saint-Béat, B., Amiraux, R., Nozais, C., Archambault, P., 2020. Reliance of deep-sea benthic macrofauna on ice-derived organic matter highlighted by multiple trophic markers during spring in Baffin Bay, Canadian Arctic. Elem. Sci. Anthr. 8. https://doi.org/10.1525/elementa.2020.047

Yunkera, M.B., Macdonaldb, R.W., Veltkamp, D.J., Cretneyb, W.J., 1995. Terrestrial and marine biomarkers in a seasonally ice-covered Arctic estuary-integration of multivariate and biomarker approaches. Mar. Chem. 49.

Zhang, Y., Dutkiewicz, S., Sunderland, E.M., 2021. Impacts of climate change on methylmercury formation and bioaccumulation in the 21st century ocean. One Earth 4, 279–288. https://doi.org/10.1016/j.oneear.2021.01.005

Appendix I. Species authorities and feeding guild references

The Arctic Traits Database (Degen and Faulwetter, 2019) provided an invaluable service in the compilation of many of the references below.

Table A.1. Species authorities, feeding guild classification and information sources for all species used in this study.

Taxon	Species Authority	Feeding Guild	Reference
Amphipoda			
Acanthostepheia behringiensis	Lockington, 1877	CV	Vedenin et al., 2015
Ampelisca sp.	Krøyer, 1842	SF	Conlan et al., 2008; McTigue and Dunton, 2014
Anonyx nugax	Phipps, 1774	CV	Nygård et al., 2012
Arctolembos arcticus	Hansen, 1887	DF	World Register of Marine Species
Paramphithoe sp.	Bruzelius, 1859	CV	Schnabel and Hebert, 2003; Stransky and Brandt, 2010
Pleustes panoplus	Krøyer, 1838	DF	Kędra et al., 2012
Rhachotropis aculeata	Lepechin, 1780	CV	Węsławski et al., 2010
Unidentified amphipod sp.		CV	Categorized by $\delta^{15}N$/trophic position
Cumacea			
Diastylidae sp.	Bate, 1856	DF	Kürten et al., 2012
Isopoda			
Munnopsis typica	Sars, 1861	DF	Wlodarska and Weslawski, 1996
Saduria entomon	Linnaeus, 1758	CV	Percy, 1983
Saduria sabini	Krøyer, 1849	CV	Conlan et al., 2008; Nelson et al., 2014; Roy et al., 2015

Taxon	Species Authority	Feeding Guild	Reference
Synidotea bicuspida	Owen, 1839	DF	Link et al., 2013; Macdonald et al., 2010
Decapoda			
Eualus gaimardii	Milne Edwards, 1837	CV	Roy et al., 2015
Sabinea septemcarinata	Sabine, 1824	DF	McGovern et al., 2018
Spirontocaris sp.	Spence Bate, 1888	CV	Macdonald et al., 2010
Pycnogonidae			
Nymphonidae sp.	Wilson, 1878	CV	Macdonald et al., 2010 ; Dietz et al., 2018
Anthozoa			
Actiniaria sp.	Hertwig, 1882	CV	Macdonald et al., 2010
Gersemia rubiformis	Ehrenberg, 1834	SF	Bergmann et al., 2009; Feder et al., 1991
Asterozoa			
Crossaster papposus	Linnaeus, 1767	CV	Bremner, 2005; Deja et al., 2016
Leptasterias spp.	Verrill, 1866	CV	Serratos, 2015
Ophiocten sericeum	Forbes, 1852	DF	Bell et al., 2016; Deja et al., 2016
Ophiacantha bidentata	Bruzelius, 1805	DF	Allen Brooks et al., 2007; Piepenburg, 2005
Stegophiura nodosa	Lütken, 1855	DF	Serratos, 2015
Holothuroidea			
Psolus sp.	Oken, 1815	SF	Macdonald et al., 2010
Nemertea			
Amphiporus sp.	Ehrenberg, 1831	CV	Macdonald et al., 2010
Sipuncula			
Unidentified sipunculid sp. A		DF*	Macdonald et al., 2010

Taxon	Species Authority	Feeding Guild	Reference
Polychaeta			
Bylgides sp.	Chamberlin, 1919	CV	Polychaeta_IOPAN Project (website); World Polychaeta Database (website)
Gattyana cirrhosa	Pallas, 1766	CV	Renaud et al., 2010
Harmothoe imbricata	Linnaeus, 1767	CV	Polychaeta_IOPAN Project (website); World Polychaeta Database (website)
Nephtys sp.	Cuvier, 1817	CV	Fauchald and Jumars, 1979; Faulwetter et al., 2014
Nereis zonata	Malmgren, 1867	DF	Macdonald et al., 2010
Pectinaria hyperborea	Malmgren, 1866	DF	Macdonald et al., 2010
Phyllodoce groenlandica	Örsted, 1842	CV	Macdonald et al., 2010; World Polychaete Database (website)
Unidentified polychaete sp.*		DF*	
Bivalvia			
Astarte spp.	Sowerby, 1816	SF	Huber, 2010
Clinocardium ciliatum	Fabricius, 1780	SF	Huber, 2010; Macdonald et al., 2010
Cyclocardia sp.	Conrad, 1867	SF	Huber, 2010
Nuculana pernula	Müller, 1779	DF	Kędra et al., 2012; Stead and Thompson, 2006
Similipecten greenlandicus	Sowerby II, 1842	DF	Divine et al., 2015
Yoldia hyperborea	Gould, 1841	DF	Huber, 2010; Iken et al., 2010; Stead and Thompson, 2006
Gastropoda			
Boreotrophon truncatus	Strøm, 1768	CV	Graham, 1998

Taxon	Species Authority	Feeding Guild	Reference
Buccinum spp.	Linnaeus, 1758	CV	Graham, 1998; Heller, 2015
Cryptonatica sp.	Dall, 1892	CV	Macdonald et al., 2010
Cylichna sp.	Lovén, 1846	CV	Macdonald et al., 2010
Margarites costalis	Gould, 1841	DF	Smith et al., 1985
Neptunea sp.	Röding, 1798	CV	Heller, 2015
Tachyrhynchus sp.	Mörch, 1868	SF	Allmon, 2011
Nudibranchia			
Dendronotus frondosus	Ascanius, 1774	CV	Macdonald et al., 2010

* though species is unknown, the feeding apparatus and similarities to other known species were used to ascribe a feeding guild

References for Appendix I

Allen Brooks, R., Nizinski, M.S., Ross, S.W., Sulak, K.J., 2007. Frequency of sublethal injury in a deepwater ophiuroid, Ophiacantha bidentata, an important component of western Atlantic Lophelia reef communities. Mar. Biol. 152, 307–314. https://doi.org/10.1007/s00227-007-0690-4

Allmon, W.D., 2011. Natural History of Turritelline Gastropods (Cerithiodea: Turritellidae): A Status Report. Malacologia 54, 159–202. https://doi.org/10.4002/040.054.0107

Bell, L., Bluhm, B., Iken, K., 2016. Influence of terrestrial organic matter in marine food webs of the Beaufort Sea shelf and slope. Mar. Ecol. Prog. Ser. 550, 1–24. https://doi.org/10.3354/meps11725

Bergmann, M., Dannheim, J., Bauerfeind, E., Klages, M., 2009. Trophic relationships along a bathymetric gradient at the deep-sea observatory HAUSGARTEN. Deep Sea Res. Part I Oceanogr. Res. Pap. 56, 408–424. https://doi.org/10.1016/j.dsr.2008.10.004

Bremner, J., 2005. Assessing ecological functioning in marine benthic communities. University of Newcastle upon Tyne.

Conlan, K., Aitken, A., Hendrycks, E., McClelland, C., Melling, H., 2008. Distribution patterns of Canadian Beaufort Shelf macrobenthos. J. Mar. Syst. 74, 864–886. https://doi.org/10.1016/j.jmarsys.2007.10.002

Coyle, K., Highsmith, R., 1994. Benthic amphipod community in the northern Bering Sea: analysis of potential structuring mechanisms. Mar. Ecol. Prog. Ser. 107, 233–244.

Degen, R., Faulwetter, S., 2019. The Arctic Traits Database – a repository of

Arctic benthic invertebrate traits. Earth Syst. Sci. Data. 11, 301–322. https://doi.org/10.5194/essd-11-301-2019

Deja, K., Węsławski, J.M., Borszcz, T., Włodarska-Kowalczuk, M., Kukliński, P., Bałazy, P., Kwiatkowska, P., 2016. Recent distribution of Echinodermata species in Spitsbergen coastal waters. Polish Polar Res. 37, 511–526. https://doi.org/10.1515/popore-2016-0027

Dietz, L., Dömel, J.S., Leese, F., Lehmann, T., Melzer, R.R., 2018. Feeding ecology in sea spiders (Arthropoda: Pycnogonida): what do we know? Front. Zool. 15, 7. https://doi.org/10.1186/s12983-018-0250-4

Divine, L., Iken, K., Bluhm, B., 2015. Regional benthic food web structure on the Alaska Beaufort Sea shelf. Mar. Ecol. Prog. Ser. 531, 15–32. https://doi.org/10.3354/meps11340

Fauchald, K., Jumars, P., 1979. The Diet of Worms : a Study of Polychaete Feeding Guilds. Oceanogr. Mar. Biol. Annu. Rev. 17, 193–284.

Faulwetter, S., Markantonatou, V., Pavloudi, C., Papageorgiou, N., Keklikoglou, K., Chatzinikolaou, E., Pafilis, E., Chatzigeorgiou, G., Vasileiadou, K., Dailianis, T., Fanini, L., Koulouri, P., Arvanitidis, C., 2014. Polytraits: A database on biological traits of marine polychaetes. Biodivers. Data J. 2, e1024. https://doi.org/10.3897/BDJ.2.e1024

Feder, H.M., Naidu, A.S., Hameedi, J., Jewett, S., Johnson, W., 1989. The Chukchi Sea continental shelf: benthos-environmental interactions. US Department of Commerce, National Oceanic and Atmospheric Administration.

Graham, A., 1988. Molluscs : prosobranch and pyramidellid gastropods : keys and notes

for the identification of the species, 2nd ed. Leiden, New York.

Heller, J., 2015. Sea Snails. Springer International Publishing, Cham. https://doi.org/10.1007/978-3-319-15452-7

Huber, M., 2010. Compendium of Bivalves. ConchBooks, Hackenheim.

Iken, K., Bluhm, B., Dunton, K., 2010. Benthic food-web structure under differing water mass properties in the southern Chukchi Sea. Deep Sea Res. Part II Top. Stud. Oceanogr. 57, 71–85. https://doi.org/10.1016/j.dsr2.2009.08.007

Kędra, M., Gromisz, S., Geringer, M., n.d. Polychaeta_IOPAN Project [WWW Document]. http://www.iopan.gda.pl/projects/Polychaeta/.

Kędra, M., Kuliński, K., Walkusz, W., Legeżyńska, J., 2012. The shallow benthic food web structure in the high Arctic does not follow seasonal changes in the surrounding environment. Estuar. Coast. Shelf Sci. 114, 183–191. https://doi.org/10.1016/j.ecss.2012.08.015

Kürten, B., Frutos, I., Struck, U., Painting, S.J., Polunin, N.V.C., Middelburg, J.J., 2013. Trophodynamics and functional feeding groups of North Sea fauna: a combined stable isotope and fatty acid approach. Biogeochemistry 113, 189–212. https://doi.org/10.1007/s10533-012-9701-8

Link, H., Piepenburg, D., Archambault, P., 2013. Are Hotspots Always Hotspots? The Relationship between Diversity, Resource and Ecosystem Functions in the Arctic. PLoS One 8, e74077. https://doi.org/10.1371/journal.pone.0074077

Macdonald, T.A., Burd, B.J., Macdonald, V.I., Van Roodselaar, A., 2010. Taxonomic and Feeding Guild Classification for the Marine Benthic Macroinvertebrates of the Strait of Georgia, British Columbia. Can. Tech. Rep. Fish. Aquat. Sci. 2874.

McGovern, M., Berge, J., Szymczycha, B., Węsławski, J., Renaud, P., 2018. Hyperbenthic food-web structure in an Arctic fjord. Mar. Ecol. Prog. Ser. 603, 29–46. https://doi.org/10.3354/meps12713

McTigue, N.D., Dunton, K.H., 2014. Trophodynamics and organic matter assimilation pathways in the northeast Chukchi Sea, Alaska. Deep Sea Res. Part II Top. Stud. Oceanogr. 102, 84–96. https://doi.org/10.1016/j.dsr2.2013.07.016

Nelson, R.J., Ashjian, C.J., Bluhm, B.A., Conlan, K.E., Gradinger, R.R., Grebmeier, J.M., Hill, V.J., Hopcroft, R.R., Hunt, B.P. V., Joo, H.M., Kirchman, D.L., Kosobokova, K.N., Lee, S.H., Li, W.K.W., Lovejoy, C., Poulin, M., Sherr, E., Young, K. V., 2014. Biodiversity and Biogeography of the Lower Trophic Taxa of the Pacific Arctic Region: Sensitivities to Climate Change, in: The Pacific Arctic Region. Springer Netherlands, Dordrecht, pp. 269–336. https://doi.org/10.1007/978-94-017-8863-2_10

Nygård, H., Berge, J., Søreide, J., Vihtakari, M., Falk-Petersen, S., 2012. The amphipod scavenging guild in two Arctic fjords: seasonal variations, abundance and trophic interactions. Aquat. Biol. 14, 247–264. https://doi.org/10.3354/ab00394

Percy, J.A., 1983. Distribution of Arctic Marine Isopods of the Mesidotea (= Saduria) Complex in Relation to Depth, Temperature, and Salinity in the Southern Beaufort Sea. ARCTIC 36. https://doi.org/10.14430/arctic2288

Piepenburg, D., 2005. Recent research on Arctic benthos: common notions need to be revised. Polar Biol. 28, 733–755. https://doi.org/10.1007/s00300-005-0013-5

Read, G., Fauchald, K., 2022. World Polychaeta Database [WWW Document]. https://www.marinespecies.org/polychaeta.

Renaud, P.E., Tessmann, M., Evenset, A., Christensen, G.N., 2011. Benthic food-web structure of an Arctic fjord (Kongsfjorden, Svalbard). Mar. Biol. Res. 7, 13–26. https://doi.org/10.1080/17451001003671597

Roy, V., Iken, K., Gosselin, M., Tremblay, J.-É., Bélanger, S., Archambault, P., 2015. Benthic faunal assimilation pathways and depth-related changes in food-web structure across the Canadian Arctic. Deep Sea Res. Part I Oceanogr. Res. Pap. 102, 55–71. https://doi.org/10.1016/j.dsr.2015.04.009

Schnabel, K.E., Hebert, P.D.N., 2003. Resource-associated divergence in the arctic marine amphipod Paramphithoe hystrix. Mar. Biol. 143, 851–857. https://doi.org/10.1007/s00227-003-1126-4

Serratos, C., 2015. Spatial and temporal patterns of epibenthic community and food web structure in the Chukchi Sea between 2004-2012. University of Alaska - Fairbanks, Fairbanks.

Smith, B.D., Cabot, E.L., Foreman, R.E., 1985. Seaweed detritus versus benthic diatoms as important food resources for two dominant subtidal gastropods. J. Exp. Mar. Bio. Ecol. 92, 143–156. https://doi.org/10.1016/0022-0981(85)90093-0

Stead, R.A., Thompson, R.J., 2006. The influence of an intermittent food supply on the feeding behaviour of Yoldia hyperborea (Bivalvia: Nuculanidae). J. Exp. Mar. Bio. Ecol. 332, 37–48. https://doi.org/10.1016/j.jembe.2005.11.001

Stransky, B., Brandt, A., 2010. Occurrence, diversity and community structures of peracarid crustaceans (Crustacea, Malacostraca) along the southern shelf of Greenland. Polar Biol. 33, 851–867. https://doi.org/10.1007/s00300-010-0785-0

Vedenin, A.A., Galkin, S. V., Kozlovskiy, V. V., 2015. Macrobenthos of the Ob Bay and

adjacent Kara Sea shelf. Polar Biol. 38, 829–844. https://doi.org/10.1007/s00300-014-1642-3

Węsławski, J., Opanowski, A., Legeżyńska, J., Maciejewska, B., Włodarska-Kowalczuk, M., Kędra, M., 2010. Hidden diversity in Arctic crustaceans. How many roles can a species play? Polish Polar Res. 31, 205–216. https://doi.org/10.2478/v10183-010-0001-5

Wlodarska, M., Weslawski, J.M., Gromisz, S., 1997. A comparison of the macrofaunal community structure and diversity in two Arctic glacial bays - a old one off Franz Josef Land and a warm one off Spitsbergen. Oceanogr. Lit. Rev. 44.

World Register of Marine Species [WWW Document], n.d.